CHALMERS
UNIVERSITY OF TECHNOLOGY

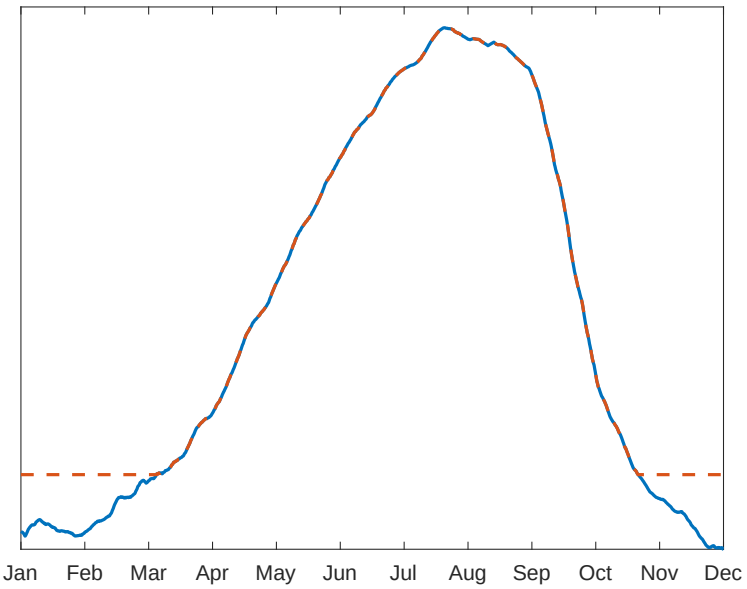


# Utilization of Industrial Excess Heat for $CO_2$ Capture

## Effects on Capture Process Design and District Heating Supply

Master's thesis in Innovative and Sustainable Chemical Engineering

ÅSA ELIASSON & ELIN FAHRMAN

Department of Space, Earth and Environment
CHALMERS UNIVERSITY OF TECHNOLOGY
Gothenburg, Sweden 2020

Master's thesis 2020

# Utilization of Industrial Excess Heat for $CO_2$ Capture

Effects on Capture Process Design and District Heating Supply

ÅSA ELIASSON & ELIN FAHRMAN


CHALMERS
UNIVERSITY OF TECHNOLOGY

Department of Space, Earth and Environment
*Division of Energy Technology*
Chalmers University of Technology
Gothenburg, Sweden 2020

Utilization of Industrial Excess Heat for $CO_2$ Capture
Effects on Capture Process Design and District Heating Supply
ÅSA ELIASSON & ELIN FAHRMAN



Supervisor: Maximilian Biermann, Department of Space, Earth and Environment
Examiner: Fredrik Normann, Department of Space, Earth and Environment

Master's Thesis 2020
Department of Space, Earth and Environment
Division of Energy Technology
Chalmers University of Technology
SE-412 96 Gothenburg
Telephone +46 31 772 1000

Cover: Available excess heat (blue) compared to reboiler duty (orange) for a seasonally varying operation of a steel mill capture plant.

Typeset in LaTeX
Printed by Chalmers Reproservice
Gothenburg, Sweden 2020

Utilization of Industrial Excess Heat for $CO_2$ Capture
Effects on Capture Process Design and District Heating Supply
ÅSA ELIASSON & ELIN FAHRMAN
Department of Space, Earth and Environment
Chalmers University of Technology

# Abstract

Carbon capture and storage (CCS) has been identified as a technology necessary to mitigate climate change and reach the 2°C target of the Paris agreement. Utilization of industrial excess heat is a way to make investments in CCS more feasible. However, in Sweden, industrial excess heat is often utilized for district heating. Thus, CCS may compete with district heating for utilization of industrial excess heat.

This thesis evaluates the potential of operating a CCS plant on excess heat from an industrial plant, that is currently utilized for district heating. A techno-economic assessment is performed to discuss design and operational modes of the capture plant. Two industrial plants are investigated as case studies, Preem's refinery in Gothenburg and the SSAB steel mill in Luleå. Two operational modes are investigated, a seasonally varying (SV) operation and a constant load (CL) operation.

If CCS is prioritized over district heating, i.e. excess heat is utilized for CCS without considering the district heating supply, 9.7% and 25.5% of the initial excess heat could be recovered for district heating after capture, for the steel mill and the refinery case respectively. The different properties of the flue gas from the two cases and the process configuration of the capture plant are important to the heat recovery potential from the capture plant.

If the district heating delivery is retained, by operating the CCS plant on either the excess heat not utilized for district heating or on primary energy, 17% of the direct $CO_2$ emissions of the steel mill plant is avoided in SV and CL. The SV operation results in that 99% of the total amount of captured $CO_2$ is also avoided. The corresponding figure for the CL operation is 93%. The two operational modes yield comparable costs, however, the SV operation is deemed most viable, since it avoids the use of primary energy, and provides a flexibility in being able to scale-up CCS operation in the future. By evaluating the economic performance of the steel mill capture plants from both parts of the thesis, it is seen that the designs and operational modes are comparable, with specific costs of 40-45 €/tonne $CO_2$ avoided. The feasibility of the alternatives are, however, dependent on how CCS and district heating are valued in relation to each other. If CCS is prioritized, and the loss of district heating revenue is not taken into account, a specific cost of 27 €/tonne $CO_2$ avoided is achievable.

Keywords: Carbon capture and storage, District heating, Excess heat, Seasonal variations, Specific cost

# Acknowledgements

We would like to express our gratitude towards our supervisor, Maximilian Biermann, who has always been there to discuss our many questions, as well as provided invaluable insights and guidance throughout the work. Max has shown an incredible interest, and also encouraged us to build on our own ideas. Additionally, Max has helped us improve the report, by providing detailed and insightful commentary.

We would also like to thank our examiner, Fredrik Normann, who has provided valuable input and interesting ideas for the work through our bi-weekly meetings, as well as constructive comments on the report.

Lastly, we would like to thank Elin Andersson and Arvid Skogström, for helpful discussions about compressors and turbines, as well as our many coffee break walks around the office.

Åsa Eliasson & Elin Fahrman, Gothenburg, June 2020

# Disclaimer

The case studies in this work are based on published literature and reports and do not claim to represent current processes accurately at the mentioned companies. Neither has there been an exchange of information with the mentioned companies in relation to this thesis.

# Contents

# List of Abbreviations

| | |
|---|---|
| AEH | Avoidable Excess Heat |
| BFG | Blast Furnace Gas |
| CAPEX | Capital Expenditures |
| CCS | Carbon Capture and Storage |
| CEPCI | Chemical Engineering Plant Cost Index |
| CHP | Combined Heat and Power |
| CL | Constant Load |
| CS | Carbon Steel |
| DCC | Direct Contact Cooler |
| DH | District Heating |
| EDF | Enhanced Detailed Factor |
| EH | Excess Heat |
| EIC | Equipment Installed Cost |
| HCC | Hot Composite Curve |
| HCN | Heat Collecting Network |
| OPEX | Operational Expenditures |
| SV | Seasonally Varying |
| TIC | Total Installed Costs |
| UEH | Unavoidable Excess Heat |
| UH | Useful Heat |
| WH | Waste Heat |

# List of Figures

# List of Tables

# 1
# Introduction

This thesis work evaluates the relation between heat supply for absorption-based carbon capture processes and district heating from industrial excess heat. For example, the work discusses whether the prioritization should be district heating delivery or to run the carbon capture plant continuously at full load. A techno-economic assessment is carried out, in which the investment cost and running cost for each configuration are estimated and compared.

## 1.1 Background

Anthropogenic activities have caused a global warming of about 1°C [1] by increasing the carbon dioxide concentration in the atmosphere from 280 ppm at pre-industrial levels [2] to more than 400 ppm at current date [3]. In 2015, the Paris agreement was signed by the parties of the United Nations Framework Convention on Climate Change. The aim of the agreement is to mitigate climate change in order to limit the global warming to well below 2°C and preferably to stabilize the global average temperature at 1.5°C above pre-industrial levels [4]. Furthermore, in 2018, the International panel of climate change (IPCC) published a special report, in which they stated multiple reasons for limiting the warming to 1.5°C rather than 2°C [1].

Different means of action to mitigate $CO_2$ emissions are available, of which one of the most important methods is to increase energy efficiency [5]. In the heating sector, one option for reducing primary energy use is the centralization of heating systems, i.e., replacing individual heating systems with district heating (DH) [6]. In Sweden, the DH network has been in use and successively expanded since the late 1940's, which has helped reducing the amount of individual oil boilers to almost zero [7], resulting both in an improvement of the air quality and emission reductions. Since the 1990's, the DH production has increased by 50% while the emissions from the sector have decreased. One reason for this is the increased use of excess heat (EH) from industrial sites to provide DH, which has led to large energy savings by increased resource efficiency [8].

A possibly competing area of use for industrial EH, which has emerged in recent years, is carbon capture and storage (CCS). CCS has been identified as a necessary technology to reach the current climate goals [1], [9]. The basic procedure of CCS means separating carbon dioxide from a large point source, and then storing it in a suitable geological formation. A major barrier for implementing CCS technology

is however the economic expense of building and running the plants [10]. Several studies have been conducted on the topic of reducing the costs [11], [12]. The CCS process is energy intensive, causing large operational expenditures (OPEX). Utilizing EH to run a CCS plant could potentially reduce OPEX, making investments in CCS more feasible. The use of EH for CCS has been investigated in several previous studies [13]–[15].

Many point sources of $CO_2$ emissions are located at industrial sites, and according to the International Energy Agency (IEA), the industry sector was responsible for about 24% of the total global $CO_2$ emissions in 2017 [16]. A major part of this sector thus requires extensive implementation of new, carbon neutral technology. Many industrial plants have access to EH, providing promising conditions for implementation of CCS. The benefits of investing in CCS have been pointed out in recent studies, where the future expense of climate change mitigation have shown to be significantly larger if little or no investments into CCS are made [9].

As previously mentioned, in Sweden, the utilization of EH for DH has played an important role in reducing carbon dioxide emissions by increasing energy efficiency. Hence, the challenge lies in finding solutions enabling both implementation of CCS and continued heat supply to the DH network. During the summer months, the demand for DH is low, providing an opportunity for CCS to be implemented. Utilizing the heat for CCS during this period could provide a way to valorize the EH that would otherwise require additional cooling. Due to the large investment cost of a CCS plant, only capturing $CO_2$ during summer will, however, cause large specific costs per tonne $CO_2$ capture, and may not be defensible from an economic point of view. The heat integration of a DH network with a CCS plant by utilizing the various coolers of the CCS plant has been investigated in previous studies, e.g. in [17]. However, the work by Bartela et al. [17] was focused on heat and power plants, whereas the focus in this thesis is industrial plants. In contrast to heat and power plants, industrial plants generates EH, i.e. does not generate heat as a main product. Furthermore, heat and power plants to some extent have the possibility to operate in a flexible manner, following the heat demand, while industrial plants more often run their production continuously throughout the year, thus providing a rather constant availability of EH.

## 1.2 Aim and scope

The aim of this thesis is to investigate how the limited amount of excess heat from an industrial plant could be distributed between DH and CCS, taking into account seasonal variations in DH demand, as well as whether extraction of heat for DH supply from the $CO_2$ separation plant is possible. The evaluation takes into account economical performance, but also factors such as the view on CCS and DH are discussed.

More specifically, by comparing two industrial plants, a steel mill and a refinery, the work aims at investigating whether characteristics such as the properties of the

flue gas affects the possibility to recover heat for DH supply from the $CO_2$ separation plant. Furthermore, the work aims at evaluating and comparing different approaches to handling seasonal variations in DH in terms of economic performance, but also the environmental consequences in terms of emissions avoidance of each option.

In this thesis, the economic evaluation is only a rough estimation. The purpose is mainly to quantitatively compare the performance of the $CO_2$ separation plants under different conditions. Additionally, the economic study is limited to evaluating the $CO_2$ separation plant including the compression units. In other words, transportation and storage, as well as costs related to the equipment for heat integration from CCS to the DH network are not considered.

# 2
# Theory

Industrial processes typically generate EH that originates from the production process. To increase energy efficiency, the EH can either be utilized internally within the production process by heat integration, or externally by integration with other heating systems or processes. In this thesis, two different external areas of utilization are of interest, CCS and DH. A definition of EH, and the considered EH utilization areas, are presented in Section 2.1, 2.2 and 2.3, respectively. To evaluate the integration of an industrial plant, the DH network and a CCS plant, two different industrial plants were investigated as case studies. The studied industrial plants are presented in Section 2.4.

## 2.1 Definition of excess heat

EH has been defined in different ways in previous studies. Broberg Viklund and Johansson [18] define EH as "heat generated as a by-product of industrial processes. This heat is not used today, but could be used to create benefits for the industry and society". Olsson et al. [19] use the definition "excess energy [is energy] that cannot be utilized internally and where the alternative is that the heat is released into the surroundings". In this thesis, the definition used by Petterson et al. [20] will be applied, i.e. EH is "the heat discharged from an industrial process". The EH can originate from chemical reactions, but it can also originate from primary energy if there is left-over heat after heat has been supplied to a certain processing step. The left-over heat might e.g. be the heat in hot effluent streams.

Furthermore, the EH is divided into two categories according to the work of Pettersson et al. [20], avoidable excess heat (AEH) and unavoidable excess heat (UEH). AEH is EH that can be avoided by internal process heat integration that is feasible from a techno-economical point of view. UEH, on the other hand, cannot be utilized internally. Thus, according to the definition used in this thesis, EH is discharged heat that is not currently utilized in the plant, but may have potential to be utilized internally, if it is AEH. The UEH will, however, always need to be cooled by either emitting the heat to the atmosphere, heat exchanging with cooling utilities or external utilization. Another option, although it might be less feasible, would be to avoid parts of the UEH by extending the heat integration of the industrial plant to reach its full thermodynamic potential.

For the purpose of this thesis, UEH is divided further into two subcategories, useful

heat (UH) and waste heat (WH). UH is heat that can be utilized externally to the production process, e.g., for DH supply or heat integration with a CCS process. WH is heat at temperature levels that are not high enough to be utilized for such external applications. Figure 2.1 visualizes the different subcategories of EH that will be applied throughout this thesis.

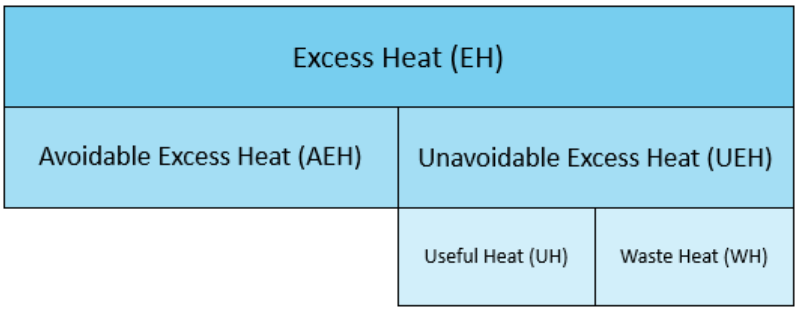


**Figure 2.1:** Illustration of the different excess heat categories applied in this thesis.

It should be kept in mind that the total amount of EH, as well as the ratio between its subcategories, will change if the internal process is modified or expanded. For example, throughout this thesis, heat integration with a CCS plant is considered an external utilization of EH. If, however, industrial plants will in the future be compelled to reduce emissions by CCS, the CCS unit might be regarded as a necessary part of the internal process, similar to other flue gas cleaning processes such as desulfurization, rather than an external plant. Thus, the heat used for CCS would then not be considered EH at all, since it is then an integrated part of the internal process.

Despite the fact that UH is the heat that in theory is wanted for DH or CCS integration, it is difficult to discern whether or not the EH that is currently used for DH is only from the UH part of EH. Without a detailed insight to the industrial plant in question, one can not tell if part of the EH utilized for DH is actually AEH which has potential to be internally heat integrated. Thus, in this thesis, the term EH will be used to denote the heat used for CCS and DH supply.

## 2.2 Carbon capture and storage

CCS can be divided into three major steps; $CO_2$ separation, transportation, and storage. In this thesis, the separation, including the pre-transport compression is mainly treated. The design of the complete chain, from $CO_2$ separation to storage, is dependent on many factors, such as the source and scale of the $CO_2$ emissions, location, and whether the plant from which the $CO_2$ originates is already in service. Several $CO_2$ separation techniques exist, such as pre- and post-combustion absorption, and oxyfuel combustion. What technique is the most suitable depends on the specifics of the plant. Generally one may prefer a technique that affects the performance of the main purpose of the plant as little as possible. Factors that may affect the choice are for example availability of heat and space.

The transport of $CO_2$ can occur by ship, train or pipeline, and the method is mainly dependent on the location of the $CO_2$ separation plant. Factors which have to be considered include how the surrounding environment may be affected by transport, but also local legislation [21]. The final storage site is also largely dependent on the location, and several options have been discussed [22]–[24]. Popular ones are oil fields no longer in use, and large underwater saline aquifers.

Carbon capture is mainly suitable for large point sources of $CO_2$, i.e., one or few gas streams carrying a large flow of $CO_2$. The opportunity to collect a large amount of $CO_2$ at one single point promotes a better economy for both separation and transport of $CO_2$, due to economy-of-scale effects [25]. Large point sources of $CO_2$ are mainly present at power plants and different types of industrial sites. This thesis focuses on the implementation of CCS at industrial sites in Sweden using the example of a refinery and a steel mill.

### 2.2.1 Absorption based carbon capture with MEA

In this thesis, post-combustion chemical absorption is the only technology considered, as it can be implemented without changing the current combustion process extensively, and is thus suitable for existing industrial plants [26]. Another advantage of post-combustion capture with chemical absorption is that it is a technology that, unlike many other technologies developed for carbon capture, has already been implemented in industry and is therefore commercially available. Chemical absorption for $CO_2$ separation has been extensively researched in academia (see for example [11], [27]) and demonstrated at commercial scale [28], [29], thus it is considered as well-proven technology.

The chemical absorption process is based on the concept of temperature-swing absorption. This means that the liquid absorbent reacts with the dissolved $CO_2$ at a low-temperature level, and is then regenerated by raising the temperature to a level where the $CO_2$ is released to the gas phase. In this thesis, the absorbent consists of an aqueous 30 wt% monoethanolamine (MEA) solution. MEA is a very efficient absorbent, and highly reactive with $CO_2$, resulting in high separation rates. Due to its other applications in industry it is already commercially available at low price levels [22]. A major drawback of MEA is the high absorption enthalpy, which causes the regeneration of MEA to be very energy intensive. In fact, the heat supply to the regeneration process is a major contributor to the cost of the CCS plant. At high temperatures and high oxygen ($O_2$) or sulphur-oxides ($SO_X$) content, MEA is also subject to degradation [22]. The levels of $O_2$ or $SO_X$ should therefore be minimized as much as possible prior to absorption, and the temperature preferably kept below 120°C in the regeneration step. As MEA is corrosive at higher concentrations, the amount has been limited to 30 wt% to avoid damage on equipment and piping.

A scheme of a post-combustion absorption plant is shown in Figure 2.2a. The flue gas first enters a direct contact cooler (DCC) which has two purposes. The first is to remove excess water from the flue gas, and the second to decrease the

temperature to a level suitable for absorption with MEA, about 40°C. The flue gas then enters the absorption column, where $CO_2$ is chemically bound to the absorbent. The temperature in the absorber usually ranges from about 40-60°C [22]. The ratio of MEA to $CO_2$ in the $CO_2$ rich solvent stream exiting at the bottom outlet of the absorber is denoted rich loading. The $CO_2$ depleted flue gas leaving the absorber enters the washer, installed on top of the absorber, where entrained MEA is removed using water. To enhance the regeneration of solvent, the pressure of the rich solvent stream exiting the absorber is increased to about 2 bar with a pump. The rich solvent stream then enters the stripper, where the MEA solvent and $CO_2$ are separated by addition of heat. The temperature is determined by pressure, usually somewhere between 100-120°C [22]. The molar ratio of $CO_2$ derivatives to MEA derivatives (lean loading) in the lean solvent flow leaving the stripper is usually around 0.2-0.3. The absorbent is recycled to the absorber, and the loss of MEA at the gas phase top effluents of the absorber and stripper via degradation is compensated with a make-up stream of MEA and water. A part of the lean solvent stream passes through a reclaimer where solvent degradation products, or heat stable salts (HSS) are removed, and is then reintroduced in the stripper. The remaining water in the $CO_2$ rich top product of the stripper is condensed and separated, and the $CO_2$ then enters the compression unit. The lean solvent stream exiting at the bottom of the column is used to preheat the rich solvent stream into the stripper via a cross heat exchanger.

Several modifications to the basic process have been investigated with the intention of reducing the heat demand of the reboiler [27], which contributes to a major part of the specific cost of the plant. Among these are the addition of an absorption intercooler (ICA), and rich-stream splitting (RSS). The modifications are illustrated in Figure 2.2b. In absorption intercooling, the fluid is extracted from a suitable stage in the absorber, cooled with a heat exchanger and then reintroduced at the stage below. ICA is suitable for gas streams with high concentration of $CO_2$ [11], [30], as high concentration causes higher temperatures and less efficient absorption. By implementing ICA, less solvent flow is required, which decreases the heat demand of the stripper reboiler. In rich stream splitting, the $CO_2$ rich absorbent stream is split into two streams before entering the stripper. One of the streams is heated and introduced at an appropriate stage, and the other is led to the top of the column without prior heating. The cold stream introduced above the hot stream promotes a more even distribution of the feed stream in the stripper, by preventing it to directly enter the condenser, effectively decreasing the heat demand of the reboiler [11].

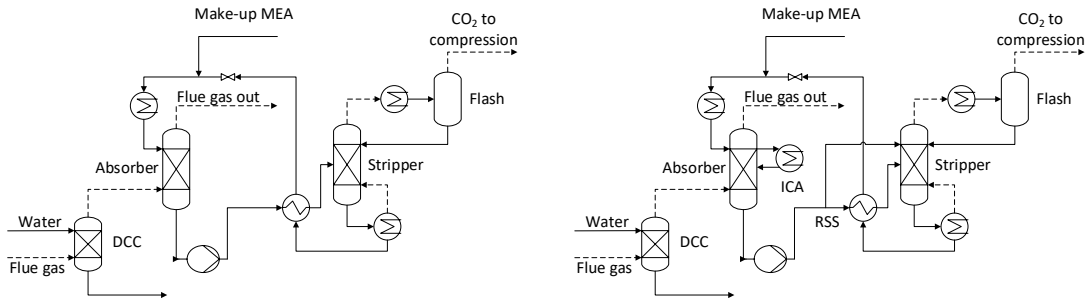


**(a)** **(b)**

**Figure 2.2:** A simplified schematic view of a post combustion $CO_2$ separation plant, without (a) and with (b) rich-stream split (RSS) and absorption intercooling (ICA).

Aside from the OPEX, the capital expenditures (CAPEX) of the post-combustion capture plant also has a large impact on the total cost. Previous studies have shown that the largest contributors to the CAPEX are the various heat exchangers, columns, and compressors [11], [31], [32]. Due to economy of scale, the total specific cost (cost/ amount $CO_2$) decreases with increasing size. Previous studies have, however, shown that above capture rates of about 90%, the specific capital cost increases [11] for absorption based post combustion capture. It is therefore, in research literature, common to define full capture as capturing 90% of the $CO_2$ of a gas stream. The capture rate is affected by a number of factors, such as liquid-to gas-ratio in the absorber, the temperature levels of the absorption and stripper columns, pressures, and the residence time and hydrodynamics as a result of the geometry of the equipment.

### 2.2.2 Compression

To facilitate transport, the $CO_2$ is compressed to a pressure which depends on the means of transportation. The two transportation methods mainly discussed are transportation by pipeline and transportation by ship. In this thesis, only transportation by ship is considered. The choice is based on a recent investigation, which has identified transportation by ship as the most feasible option in Sweden [21]. Commonly, studies investigating transportation by ship adopts a pressure between 7 and 15 bar [33], [34]. In this thesis, transportation pressure of 7 bar(a) will be used, since the practical implementation of this pressure currently being considered [35]. A schematic view of the compression plant is shown in Figure 2.3 [34].

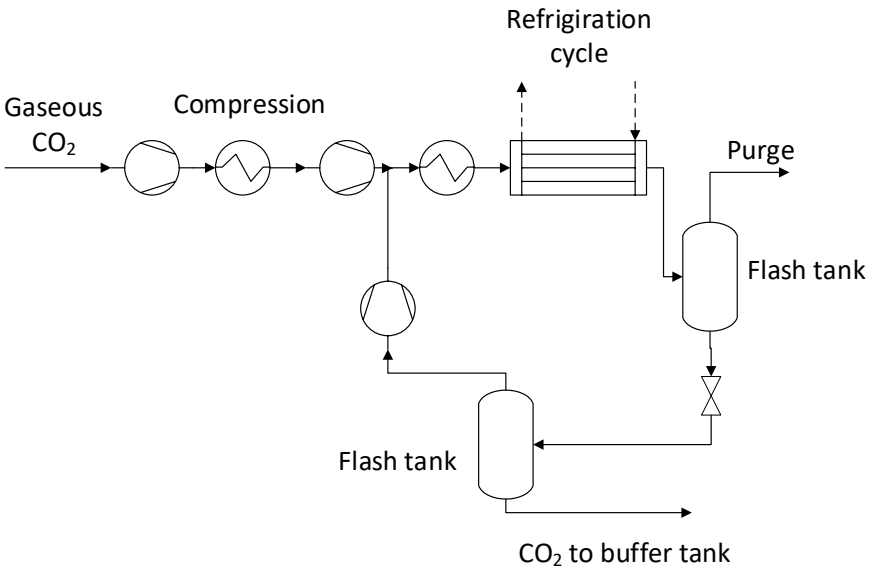


**Figure 2.3:** Schematic view of the compression and liquefaction plant, adapted from [34].

To transport $CO_2$ efficiently it has to be liquefied. With a transportation pressure of 7 bar(a), a suitable temperature is about -50°C. To avoid the high costs associated with cooling at such low temperatures, the gas is first compressed to a higher pressure than 7 bar(a), enabling liquefaction at higher a temperature. The liquefied $CO_2$ is then throttled to 7 bar(a). The optimal liquefaction pressure is a trade-off between the expense of the cooling cycle and that of the additional compression. Deng et al. have suggested a liquefaction pressure of 20 bar(a), for a delivery pressure of 7 bar(a) [34]. As per general recommendation based on the pressure ratio of 10 [36], two compressors are used. Between the compressors, the $CO_2$ is cooled to 25°C. After the gas has been compressed, impurities are removed, and cooling to liquefaction temperature is then performed with an ammonia refrigeration cycle. After liquefaction, additional impurities are purged using a flash tank, where after the gas is expanded to reach the final temperature and pressure. The gas fraction of $CO_2$ which may emerge at this stage is re-compressed and recycled. The liquid fraction is sent to a buffer tank, awaiting transportation and storage.

## 2.3 District heating

In Sweden, DH supplies about 50% of the heating demand in commercial and residential buildings. The dominating technologies for DH production are combined heat and power (CHP) plants and boilers. Combustion of biomass for heat production has increased substantially since the 1990's, and is now the most common energy source for DH. Since the ban of landfills for municipal waste in the early 2000's, the heat generation from combustion of waste has also increased to now being the second most utilized energy source. Industrial EH, including heat recovery from excess gases, contributes with about 10% of the supply [7]. However, as

previously mentioned, the utilization of industrial EH provides an important way of increasing energy efficiency [8].

DH systems consist of one or several large and centralized heat production plants and a network of underground pipes that distributes the heat in the system using medium temperature pressurized water as heat carrier. Heat from the water is supplied to the buildings in the network through individual heat exchangers in each building. The supply temperature is usually around 90°C and the return temperature is around 50°C, however these temperatures varies seasonally due to variations in outdoor temperature [7], [18].

There are different ways of recovering heat from industrial plants to provide DH. In this thesis, two different options will be considered. The first one is to collect the EH from hot gas or liquid streams by heat exchanging towards hot-water heat collection network, which thereafter supplies heat to the DH system. The second option is to utilize energy-rich waste gases as fuel in a CHP plant, which is common for integrated steel mills and the petrochemical industry. Regardless of which heat recovery option is used, the DH demand has a strong seasonal variation, meaning that the DH delivery from industrial plants is often adapted in respect to these demand-side changes. Thus, since the operation of the industrial plants does not follow the seasonal variation but is rather constant, other ways of cooling the EH on the process-side are needed when the DH demand and, thus, its provided cooling, is low.

## 2.4 Studied industrial plants

In this thesis, two industrial plants are investigated and compared, the Preem Refinery in Gothenburg and the SSAB steel mill in Luleå. The steel mill is also connected to Lulekraft, a CHP plant. SSAB steel mill and Lulekraft are in this thesis treated and evaluated as one single plant. The refinery and the steel mill are interesting to this thesis for a number of reasons. Firstly, the iron and steel industry accounts for about 24% of $CO_2$ industrial emissions globally [37], while the chemical and petrochemical industry accounts for about 10% [38], thus, making them two of the largest sources of $CO_2$ emissions. The steel mill and the refinery are also interesting because these plants, in many aspects, present two very different cases. The economic feasibility of a CCS plant may be affected by purely technical factors such as properties and composition of the flue gas to be purified. For example, the $CO_2$ concentration of the flue gas from the steel mill is substantially higher than that of the refinery. Other factors that may affect the $CO_2$ separation efficiency, and that differs between the plants, are flue gas temperature and pressure. The properties of the flue gas of each plant are presented more in detail in Chapter 3.

The extraction of DH also differs between the plants. At Preem's refinery, the DH is provided by various hot streams in the process. The heat is delivered at two different temperature levels, 90°C and 140°C. The respective return temperatures are 50°C and 90°C. A lot of the EH utilized in the DH network is provided by streams with

temperatures lower than those required to run the reboiler of the $CO_2$ separation plant. This means that not all EH currently used for DH may be utilized to power the stripper reboiler of the CCS plant. Where the steel mill is concerned, steam extracted from the turbine of the CHP plant is used to heat the DH water. As the steam extraction point in the turbine of the CHP plant could potentially be modified to occur at higher pressures, all DH may potentially be lifted to a temperature level sufficient to power the reboiler of the CCS plant, which operates at about 120°C. In the CHP plant, EH is also utilized to produce electricity. This potentially impose problems if a new extraction point is introduced, since the electricity production may be affected, depending on how much is extracted.

### 2.4.1 SSAB steel mill and Lulekraft

SSAB steel mill located in northern Sweden is used as a reference case for a typical blast furnace steel mill. The raw material of steel production is iron ore, which is reduced to pig iron using coke and coal. The reduction takes place in the blast furnace [39], and during the process, a large amount of energy-rich gases are produced as a byproduct. The gas is used as fuel to provide process heat to the steel mill and to fire the Lulekraft CHP plant [39]. A fraction of the gas is also flared during periods where the amount of gas exceeds the capacity of the CHP plant. The vast majority (98%) of the carbon that enters the steel mill leaves the plant in the form of $CO_2$. The CHP plant is the largest emission source, accounting for 59.4% of the total emissions. The hot stoves heating the air supplied to the blast furnace account for 22.3%, while the flare accounts for 10.4%. The major part of the gases combusted in these three units originates from the blast furnace [31]. When the gases leave the blast furnace, it already contains a significant amount of $CO_2$. The total amount of emissions from the plant are around 3.4 Mton$CO_2$/year [31].

The steam that is produced in the CHP plant is used for power generation, but also partly utilized internally in the steel mill and partly to supply DH to the local community [39]. The Lulekraft CHP is the main source of heat for the local DH system, with other sources only being utilized during especially cold weather, or during temporary shut down [40]. According to Lulekrafts own webpage, the DH delivery results in a yearly reduction of 204 kton of $CO_2$ equivalents [41], compared to if the heat was instead supplied by oil boilers. The electricity produced in the CHP is used to supply the mill, but is also connected to the national grid.

### 2.4.2 Preem's refinery in Gothenburg

Preem's refinery in Gothenburg is a hydro skimming refinery with a crude oil capacity of 6 Mt/year [22], [42], and is used as a reference case for an oil refinery. By atmospheric distillation, crude oil is separated into hydrocarbon fractions by addition of heat. To enhance the properties of the fractions, some additional processing is carried out, e.g. removal of sulfur and aromatic content and reforming to increase the octane number [43]. Useful fuels, such as LPG, gasoline, jet fuel, diesel and fuel oil, are produced by blending different types of hydrocarbon fractions with each

other and some additives [44].

In multiple steps of the processing, non the least the crude oil distillation, addition of heat is needed to carry out the various unit operations. Therefore, heat is produced in different units, mainly by combustion of refinery fuel gas, produced on-site, and additional natural gas. The flue gases from the heat generation units are collected and emitted to the atmosphere through two chimneys [44]. The total amount of $CO_2$ emitted from the refinery is about 0.5 Mton/year, of which 89% originate from the chimneys [22], [45]. Except for the emissions through the chimneys, $CO_2$ is also emitted through flaring of excess gases, i.e. of gases that cannot be utilized in further processing. In different steps of the process, EH is produced. EH at various temperature levels is collected from hot streams by heat exchanging towards a hot-water based heat collecting network (HCN). The heat from the heat collection network is thereafter transferred, also by heat exchanging, to the two DH systems. During the summer, when the DH demand is low, the hot streams are instead cooled by air fans [43], [44].

# 3
# Methodology

Figure 3.1 shows a schematic overview of the methodology applied in this thesis. Two different parts of the thesis were defined. In Part 1, CCS was prioritized in receiving industrial EH, meaning that as much heat as was considered available was utilized for CCS operation, without consideration to changes in DH supply. In Part 2, a retained DH supply was prioritized over capturing as much $CO_2$ as possible, meaning that the CCS plant only received EH whenever the DH demand was lower than the total amount of available EH. For both parts, only EH that is today utilized for DH supply was considered available for CCS operation, i.e., no other sources of EH from the industrial plant were considered.

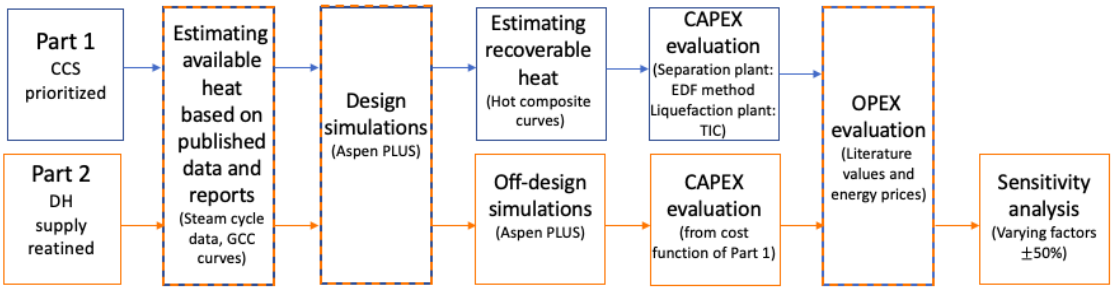


**Figure 3.1:** Flow sheet overview of the methodology applied in this thesis. The blue path represents Part 1, while the orange path represents Part 2.

In Section 3.1 and 3.2, Part 1 and 2 are described in further detail. The specifications of the heat integration, i.e. estimation of available heat as well as estimation of recoverable heat, are described in Section 3.3. The setup, including inputs, targets and outputs of the simulations carried out in the software Aspen PLUS are described in Section 3.4. Most of the approaches were simulated in design mode, i.e., the specifications of the simulation were used to size the equipment of the process. These simulations are referred to as ”design simulations”. In all the design simulations, the $CO_2$ separation plant was designed to reach a $CO_2$ separation rate of 90% in the absorber. The separation rate is defined as the ratio of $CO_2$ absorbed in the liquid in the absorber, to the $CO_2$ entering the absorber with the flue gas.

In some of the simulations, the design was fixed, i.e., the dimensions and thus the size of the plant were maintained, and the simulations were run on conditions other than the design specifications, to evaluate the off-design performance. These simulations are referred to as ”off-design simulations”, and in these the separation

rate was consequently below 90%. In total, the different approaches of CCS integration resulted in eight different designs of the CCS plant. The method used for the economic evaluation of these designs is presented in Section 3.5.

## 3.1 Part 1: Prioritizing EH supply to CCS over DH delivery

In this part of the project, CCS operation was prioritized over DH supply. To prioritize CCS means to utilize as much of the available excess heat for the $CO_2$ separation plant as possible. The amount of EH delivered to the DH system was thus reduced. The plant is operated at constant capacity throughout the year. This type of operation is interesting in a situation where CCS has to be prioritized, for example due to legislation, or high carbon emission prices. Both the SSAB steel mill and Preem's refinery were investigated as case studies and compared to investigate the influence of the different characteristics of the industrial flue gases, such as flow rate, composition, temperature and pressure. Hereinafter they will be referred to as "the steel mill case" and "the refinery case" respectively.

Three sizes (designs) of the CCS plant for each of the studied industrial plants (the steel mill case and the refinery case), were simulated and evaluated, denoted maximum size, mean size and minimum size. The maximum size was designed based on the maximum amount of available heat, as further described in Section 3.3. The minimum size was designed to obtain a total amount of captured $CO_2$ of 100 kton/year,which was deemed a limit below which CCS implementation is least likely. The mean size was designed to capture the mean amount of yearly captured $CO_2$ of the maximum and minimum sizes. All sizes were designed to obtain a 90% separation rate in the absorber, which was achieved by adjusting the flue gas flow and the solvent flow.

For the maximum sizes, the amount of heat that can be recovered from the CCS plant and used for DH supply was estimated, as described in Section 3.3. By comparing the amount of heat used for CCS, i.e. reboiler duty, and the amount of recoverable heat from CCS to the DH demand curve, the effects on the DH deliveries were estimated. All of the sizes were evaluated by economic performance, according to the method described in Section 3.5. The results from the sizes were then compared to investigate the effects of economy of scale. For the steel mill case, a cost function of CAPEX depending on plant size was formed and used in the economic evaluation of Part 2.

## 3.2 Part 2: Prioritizing retained DH supply over capturing as much $CO_2$ as possible

In this part of the project, only the steel mill case was considered. The currently practiced level of DH delivery was maintained when integrating a CCS plant, meaning that the CCS plant was assumed to operate on only the heat that was not consumed by the DH network. A retained DH delivery was thus prioritized over capturing as much $CO_2$ as possible. Two approaches to achieve this, i.e. two modes of operation of the CCS plant, were investigated. In the first mode, denoted the "seasonally varying (SV) plant", operation of the CCS plant varies seasonally, following the load curve of available heat as defined by the DH demand. In the second mode, denoted the "constant load (CL) plant", the CCS plant runs at a constant load, with an equal annual $CO_2$ avoidance as the SV plant. The $CO_2$ avoidance is in this thesis defined as the yearly amount of $CO_2$ captured, subtracted by the direct $CO_2$ emissions from the utilization of primary heat sources - assumed to be natural gas. The heat supplied to the CCS process in the two operational modes was either EH that would not be utilized due to low DH demand, or heat supplied by primary energy. The method of determining the amount of heat available for CCS for the two operational modes is described in Section 3.3.3.

In the SV plant operational mode, the process was sized to have a reboiler duty corresponding to the peak load of heat available for CCS. Thus, during the summer period, when the amount of non-utilized heat is at its highest since the DH demand is low, the capture plant was assumed to run on maximum capacity. During the rest of the year, the process was assumed to run on conditions other than its design specifications, i.e. off-design conditions, to minimize the changes to the original DH supply. To be able to evaluate the off-design performance for all levels of available heat, a number of off-design simulations were run. The results from these simulations were thereafter used to calculate the total $CO_2$ captured over the course of a year. During winter time, when the amount of available heat was close or equal to zero, the capture plant was assumed to operate at a minimum heat level. The plant of the CL operational mode was designed to operate at a constant heat level during the entire year, which was chosen to fulfill the criteria that the CL plant should obtain the same yearly $CO_2$ emission avoidance as the SV plant. For both plants, the heat deficit during winter time was compensated for by combustion of natural gas.

The CAPEX for the plants were estimated based on the cost functions developed in Part 1 of the thesis. The OPEX were evaluated according to the method described in Section 3.5.2, whereupon the economic performance was compared between the plants. Furthermore, a sensitivity analysis was carried out, as described in Section 3.5.3. A comparison was also made between the performance of the plants described in this section, where DH supply was prioritized, and the plants described in Section 3.1, where CCS was prioritized.

## 3.3 Heat integration of the $CO_2$ separation plants with the industrial plants and district heating networks

In this thesis, the investigation of heat integration has been limited to quantifying theoretical amounts of heat, and the feasibility of an actual integration network was thus not taken into account. Figure 3.2 schematically describes the different aspects to heat integration investigated. Two separate integration networks, one between the industrial plant and the $CO_2$ separation plant, and one between the separation plant and the DH network, were defined in addition to the existing one between the industry and DH network.

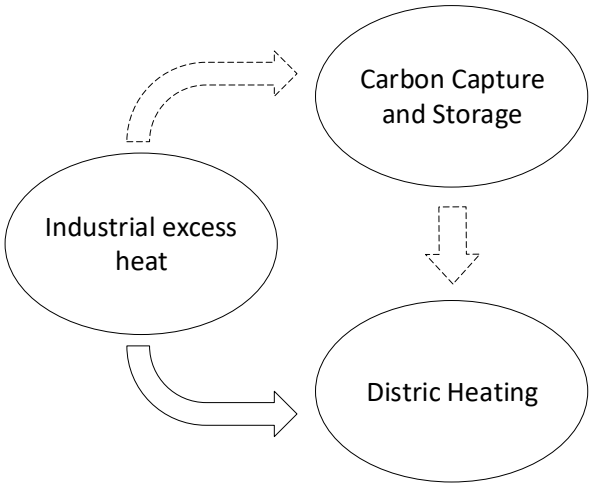


**Figure 3.2:** Schematic view of the different aspect to heat integration treated in this work.

The amount of EH considered available to the separation plant was limited to the available amount of DH, as defined for both industrial cases in Section 3.3.1, 3.3.2 and 3.3.3, as well as the temperature of the stripper reboiler. Initial simulations showed that the temperature in the stripper reboiler was about 121°C. A minimum $\Delta$T of 4°C was deemed appropriate between the hot and cold stream in the reboiler [46], thus, the hot stream had to be at least 125°C. Where the integration between the capture plant and the DH network was concerned, a minimum temperature difference of 10°C was deemed appropriate [47], and the DH water was assumed to be heated from 50°C to 90°C.

The quantification of heat that could be utilized for DH was performed by constructing a hot composite curve (HCC) of all streams in the CCS plant requiring external cooling, and adding the cold composite curve of the DH water. All coolers considered for the construction of the HCC are displayed in Figure 3.3. The condensate of the steam used to power the stripper reboiler is also a potential source of heat for DH, however, cooling of the condensate means that it also needs to be

reheated before reentering the reboiler, utilizing heat which can directly be used for DH. A cooling demand of the condensate was thus not included.

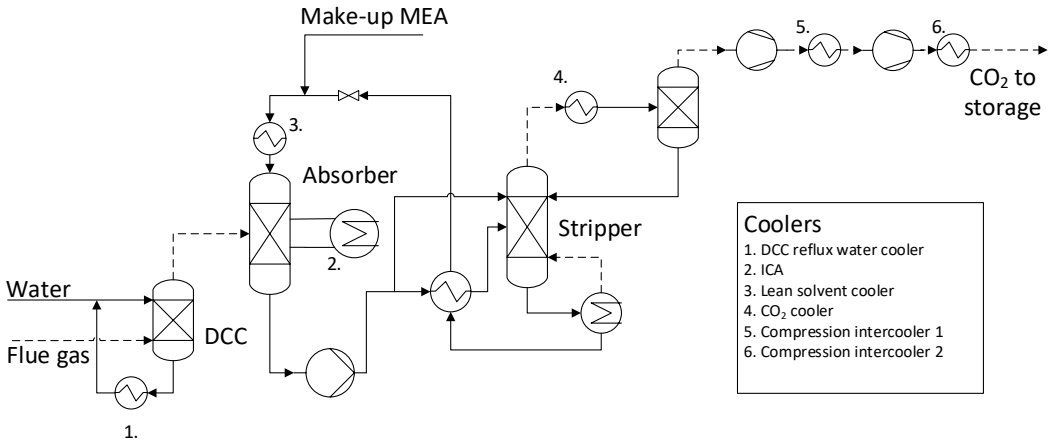


**Figure 3.3:** The process coolers considered for the construction of the hot composite curve of the CCS plant.

By comparing the heat supplied to the reboiler and the amount of recoverable heat from CCS to the DH demand curve, the effects on DH delivery was estimated. The loss was estimated by comparing with a specific reference year, assuming the same amount of operating hours for the $CO_2$ separation plant as for the industry of that specific year, which was 8760 h in both the refinery and the steel mill case.

### 3.3.1 Part 1: The refinery case

In the refinery case, a heat collecting network (HCN) is utilized to collect EH from several process streams. The minimum $\Delta T$ between the HCN and the process streams was assumed to be 5°C, thus, a total temperature difference of 9°C between the reboiler and the hot streams was assumed in the refinery case [46]. It was thus concluded that EH at a temperature of 130°C or more would be available to provide heat for the CCS process. The DH network of the refinery is divided into two partly interconnected systems, one providing heat to GEAB at 90°C (low temperature network) and one to Volvo at 140°C (high temperature network), with respective return temperatures of 50°C and 90°C. The estimation of the maximum amount of available heat in the refinery case was based on a previous screening of the DH network [47], and was determined for the high and low temperature networks separately, by utilizing the grand composite curves of the respective system (Appendix A). This showed that about 11 MW from the low temperature network, and 27 MW from the high temperature network was available at temperatures above 130°C, which resulted in a combined contribution of about 38 MW of heat [47]. Since the data of the previous screening is quite old (2008) it was compared to more recent (but less detailed) data on the monthly DH delivery of 2017 and 2018 [44], [48]. The monthly delivery showed a peak DH supply of 59 MW to the high temperature network and 40 MW to the low temperature network, agreeing well with the screening from 2008,

indicating 61 MW and 39 MW available heat at sufficient temperature respectively.

Figure 3.4 displays the monthly DH supply to the low and high temperature networks (separately and combined) for 2018, which was used as a reference year in the calculation of DH loss due to heat integration in the refinery case. The curves were calculated based on data of total amounts of heat delivered to each system as well as the operational hours of each month [44], and was assumed to be constant during a specific month. The total DH supply of 2018 was 561 GWh, of which 200 GWh was supplied to the high temperature network, and 361 GWh to the low temperature network. The 361 GWh delivered to the low temperature network accounts for about 10 % of the total DH supply from GEAB to the local community in 2018 [49].

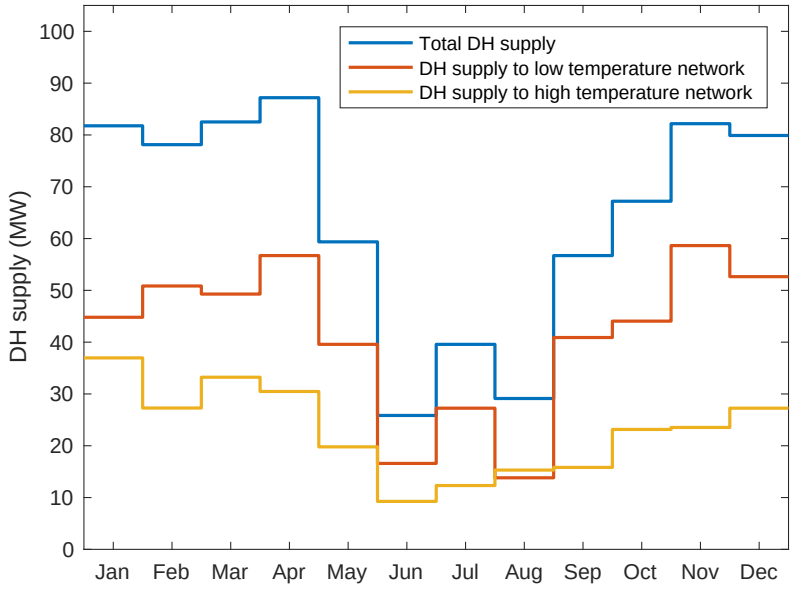


**Figure 3.4:** DH delivery from Preem's refinery in Gothenburg for the year 2018 adapted from [44]. The total delivery as well as the delivery to the high and low temperature networks is shown.

### 3.3.2 Part 1: The steel mill case

To estimate the maximum amount of available heat in the steel mill case, it was assumed that the heat extracted from the CHP turbines utilized for DH could be extracted at a somewhat higher temperature to be utilized for CCS instead. The DH supply curve of the year 2017 is presented in Figure 3.5. The curve has been smoothed to only display larger trends, thus excluding e.g. daily variations. The peak load during winter is about 160 MW, and the minimum load during summer is around 30 MW. The total DH supply of 2017 was 850 GWh.

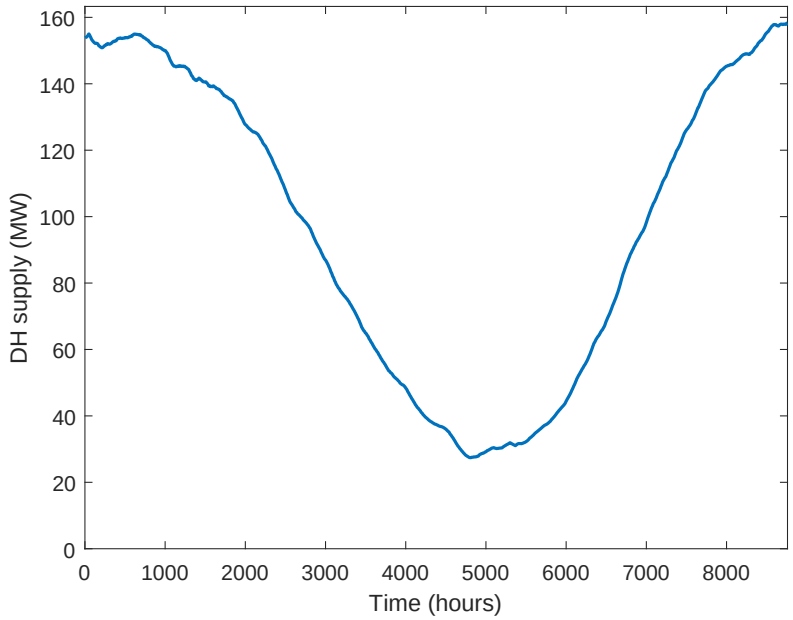


**Figure 3.5:** District heating delivery from the steel mill CHP plant Lulekraft for the year 2017. Adapted from [50].

The steam extracted from the turbines was assumed to be used directly in the stripper reboiler of the CCS plant, and a steam temperature of 125°C was thus applied to achieve a $\Delta$T of 4°C. However, since the amount of latent heat is a function of the saturation temperature of steam , the ratio of the evaporization enthalpy at the DH temperature level to the evaporization enthalpy at CCS temperature level was used to convert the heat output for DH to heat output for CCS. By the conversion calculation, it was concluded that up to 150 MW of heat could be utilized for CCS if steam was extracted at a temperature level of 125°C.

### 3.3.3 Part 2: The steel mill case, seasonally varying operational mode and constant load operational mode

To design a capture plant capable of seasonally varying operation, the difference in heat load between the minimum and maximum DH delivery was determined, considering the adaption to a higher temperature level for CCS heat as described in Section 3.3.2. Since the DH supply was retained in the second part of the thesis, the relative difference between maximum and minimum DH supply load was determined as maximum available heat for CCS in seasonally varying mode, which corresponds to a reboiler duty of up to 125.3 MW. Furthermore, the amount of heat available for CCS varied over the year in accordance with the curve displayed in Figure 3.6, which shows the temperature-level adapted and flipped DH supply curve, i.e. the CCS heat availability curve over the year.

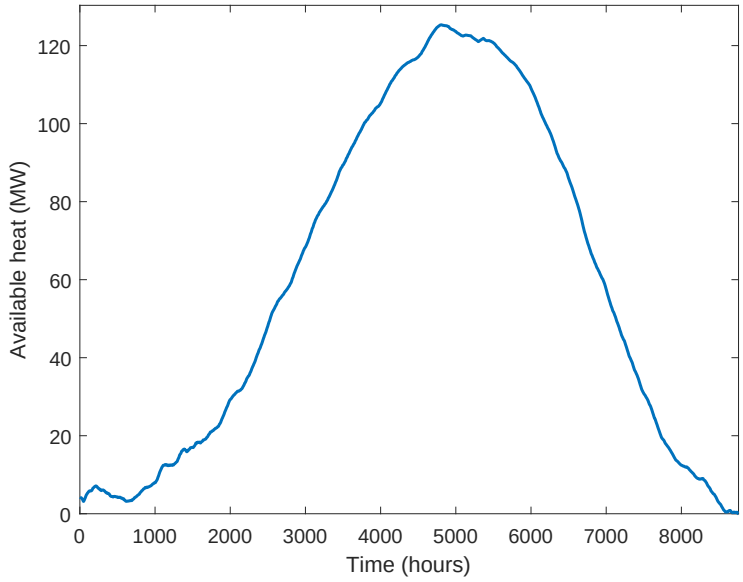


**Figure 3.6:** Seasonally varying amount of available excess heat for CCS in the steel mill case.

Martinez Castilla et al. [51] argue that it may be more beneficial to operate a capture plant on a low level of heat, to keep the plant hot, rather than having to shut down the plant entirely, especially if the heat is provided from excess heat. Therefore, a minimum heat level of 17.9 MW was assumed. In attempt of determining a minimum heat level, the idea was to determine a minimum wetting and pressure drop of the packed columns of the capture plant. However, at very low solvent flow rates, the simulation model turned out to have convergence issues. Hence, the minimum heat level was set to be the one obtained at the lowest possible solvent flow rate while the simulation still reached convergence. Evaluation of this level showed that the absorber had a separation rate of 12%, which was deemed to be a suitable minimum level of operation.

For the SV operational mode, as well as for the CL operational mode, heat from combustion of natural gas was assumed to compensate for the EH deficits during some periods of the year. The natural gas combustion plant used for compensation of the heat deficit was not specified in detail, however a fuel-to-heat efficiency of 90% was assumed, and a carbon emission factor of 50 $gCO_2/MJ_{fuel}$ [52].

The size of the CL plant was determined by iteration. The starting value was based on the constant mass flow of $CO_2$ calculated from the $CO_2$ avoidance of the SV plant. The corresponding reboiler duty was determined and the total heat deficit over the year as well as extra emissions from natural gas was calculated. The extra mass flow of $CO_2$, corresponding to the amount of $CO_2$ from combustion of natural gas, was added to the original mass flow. Thereby, a new reboiler duty was obtained. The iteration was completed when the latest obtained reboiler duty was the same as the one in the previous loop of iteration.

## 3.4 Modeling in Aspen PLUS

All simulations were carried out in the software Aspen PLUS V11. The model of the capture process itself has already been built prior to this thesis [30]. However, as described below, in this thesis a compression sequence has been added to be able to fully estimate the amount of heat that can be recovered and utilized for DH.

### 3.4.1 Simulation setup

The principal setup of the simulated process is presented in Figure 3.7. Stream names are marked with a frame, while equipment names are those without frames. "FG" stands for flue gas, "RICH" implies streams rich in $CO_2$ and "LEAN" denotes streams lean of $CO_2$.

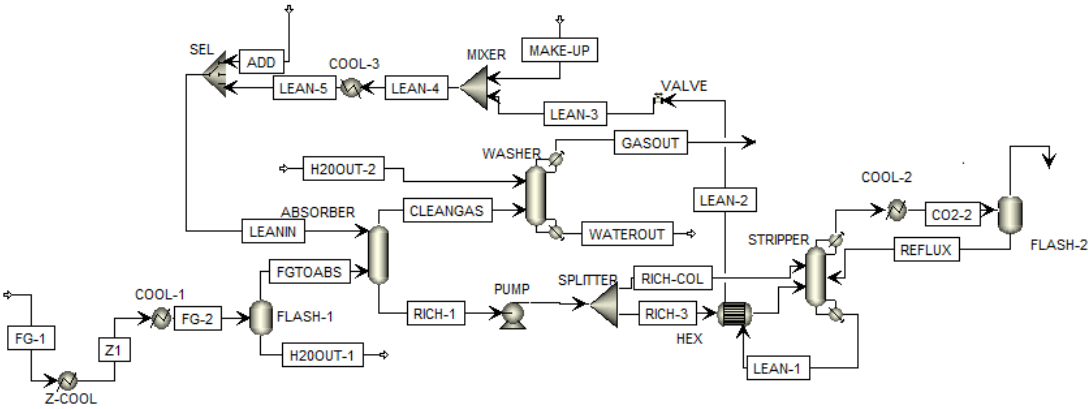


**Figure 3.7:** Aspen PLUS model of the simulated CCS plant.

Data of the composition, temperature, pressure and flow rate of the flue gases were used to define the industrial flue gas stream in the simulations, and are displayed in Table 3.1. In the steel mill simulations, the flue gas was defined as the blast furnace gas (BFG). Due to the elevated pressure in the BFG, the specific heat demand in the stripper reboiler has shown to be significantly lower compared to capture of $CO_2$ from the CHP flue gases at atmospheric pressure [31]. In the refinery case, the $CO_2$ separation plant was integrated after the two main chimneys, as these account for 89% of the direct emissions from the plant. The flue gas composition of the two stacks was not completely known, and therefore had to be estimated for all components except $CO_2$ [22]. Most of the flue gas originates from combustion of fuel gas, an energy rich by-product gas produced in various process units. The composition of the flue gas was calculated based on the assumption that the fuel gas composition was similar to that of natural gas, and combusted with 12% excess air, but the actual amount of $CO_2$ was kept. In Table 3.1, the properties of the separate chimneys as well as the combined properties are shown.

The amount of flue gas that could be purified is limited by the amount of available heat as defined in Section 3.3. In the refinery case, initial simulations showed

that the 38 MW of heat available corresponds to purifying 234 kNm$^3$/h, about 74% of the total flow to 90%. Thus, in the refinery case, the amount of available heat was the limiting factor for the maximum size of the separation plant. In the steel mill case, however, 150 MW was available, but only around 133 MW of heat was needed to power the reboiler when capturing the full BFG flow at 90% capture rate. Thus, the maximum size was instead limited by the amount of flue gas.

**Table 3.1:** The properties of the flue gases of the steel mill case and the refinery case [22], [31].

| | **Refinery case** | | | **Steel mill case** |
|---|---|---|---|---|
| | **Chimney 1** | **Chimney 2** | **Total** | **BFG** |
| **$CO_2$ [mol%]** | 8.7 | 9.0 | 8.9 | 24.6 |
| **$N_2$ [mol%]** | - | - | 71.1 | 49.6 |
| **$H_2O$ [mol%]** | - | - | 2.0 | 2.2 |
| **CO[mol%]** | - | - | 0 | 20.4 |
| **$H_2$ [mol%]** | - | - | 0 | 3.2 |
| **$O_2$[mol%]** | - | - | 2.0 | 0 |
| **Temperature [°C]** | 150 | 180 | 168 | 29 |
| **Pressure [bar]** | 1.01 | 1.01 | 1.01 | 1.81 |
| **Total flow [kNm$^3$/h]** | 128 | 189 | 317 | 352 |
| **Simulation input flow [kNm$^3$/h]** | - | - | 234 | 352 |

In Table 3.2, the basic settings of the simulations of the refinery case and the steel mill case are shown. In the capture plant, three columns with structured packing were simulated, an absorber, a washer and a stripper. In reality, however, the washer is the top part of the absorber, but to enhance the simulations, it is modeled separately. All columns are packed with structured packing of the type Sulzer Mellapak 250Y. The separation in all three columns is modelled through rate-based calculations. The height of the stripper and the absorber were set to 15 m and 20 m respectively, and kept fixed in all simulations, while the diameter of the columns was calculated. The diameter of the washer was set to the same as that of the absorber, while the height was calculated.

In the absorber, the operating pressure was set to match the pressure of the flue gas in each respective case. A higher operating pressure is favorable for the absorption, however not favorable enough to pressurize a flue gas of low pressure. The feed temperature to the absorber was set to 40°C in the refinery case, a commonly used temperature. However, a somewhat lower temperature level is acceptable, and it was thus deemed unnecessary to heat the flue gas of the steel mill case, which was kept at 29°C. The lean solvent entering the absorber was set to the same temperature as the flue gas in the respective case. For the stripper, the lean loading was used as design parameter, and set to 30 mol%. The lean loading is defined as the ratio of $CO_2$ derivatives to MEA derivatives in the lean solvent flow.

In the steel mill case, due to the already low flue gas temperature, and that the

water content in the flue gas is very low, the DCC was excluded. However, ICA was included, as the $CO_2$ concentration of the flue gas is quite high [11]. The flue gas from the refinery presented a relatively low $CO_2$ concentration, about 8.9%. As ICA is mainly suitable for gas streams with higher $CO_2$ concentrations, ICA was excluded from this process model. RSS was implemented in both cases.

**Table 3.2:** Simulation setup specifications for the refinery case and the steel mill case respectively.

| | **Refinery case** | **Steel mill case** |
|---|---|---|
| Lean loading | 30 mol% | 30 mol% |
| Absorber packing height | 20 m | 20 m |
| Stripper packing height | 15 m | 15 m |
| Stripper overhead pressure | 2 bar(a) | 2 bar(a) |
| Lean/rich cross heat exchanger $\Delta$T hot inlet/cold outlet | 10°C | 10°C |
| Lean solvent temperature into absorber | 40°C | 29°C |
| Lean solvent pressure into absorber | 1.01 bar | 1.81 bar |
| ICA | No | Yes |
| RSS | Yes | Yes |
| DCC | Yes | No |
| Discharge pressure compressor 1 | 6.3 bar(a) | 6.3 bar(a) |
| Discharge pressure compressor 2 | 20 bar(a) | 20 bar(a) |
| Intercooling exit temperature | 25°C | 25°C |

For the purpose of this thesis, a compression sequence including intermediate cooling was added to the simulation model, which is shown in Figure 3.8. The stream entering the compression sequence is the $CO_2$-rich gas outlet from the unit denoted FLASH-2 in Figure 3.7. In Figure 2.3, the full compression and liquefaction plant was illustrated. However, only the compression part was modeled, i.e. the compression of $CO_2$ to 20 bar, since that is the part of interest for the potential integration with the DH system. The compressors were modeled with an isentropic efficiency of 0.85 [34], and the equation of state used in the compressor sequence was Peng-Robinsson with Boston-Mathias extrapolation [53]. The intercoolers (COOL-4 and COOL-8) cools the $CO_2$ to 25 °C. After each cooler a knock out drum is used to remove excess water.

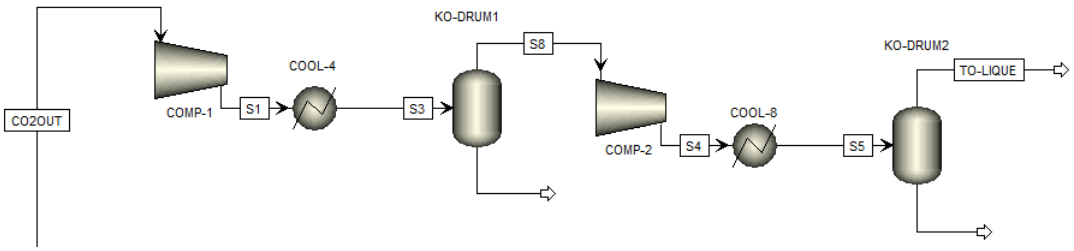


**Figure 3.8:** Modeled compression sequence.

### 3.4.2 Simulation and output

In Table 3.3 the simulation targets for each of the on- and off-design simulations have been collected. The lean solvent flow rate was adjusted to obtain the desired separation rate of 90% in the absorber in all design simulations. To obtain a specific reboiler heat, capture rate (ktonCO$_2$/year) or CO$_2$ avoided, the flue gas flow was also adjusted. Only the SV operation design was also simulated in off-design. In this case, the separation rate in the absorber was reduced by decreasing the lean solvent flow rate, while maintaining the column geometries in absorber and stripper. All other design parameters were specified in the same way as on-design (cf. Table 3.2).

**Table 3.3:** Design variables and targets for all simulations. The SV design of part 2 was the only design also simulated in off-design mode.

| **Part 1.** | **Adjusted** | **Target** |
|---|---|---|
| Refinery maximum case | Flue gas and lean solvent flow rate | Available EH (38 MW) |
| Steel mill maximum case | Lean solvent flow rate | 90% of BFG CO$_2$ captured |
| Mean case, refinery and steel mill | Flue gas and lean solvent flow rate | Yearly capture rate mean case |
| Minimum case, refinery and steel mill | Flue gas and lean solvent flow rate | Capture rate 100 kton/year |
| **Part 2.** | **Adjusted** | **Target** |
| SV operation | Flue gas and lean solvent flow rate | Maximum availability of heat (125.3 MW) |
| SV operation, off-design | Lean solvent flow rate | Available EH (varying) |
| CL operation | Flue gas and lean solvent flow rate | Same amount of CO$_2$ avoided as SV operation |

To evaluate the off-design performance of the SV operation of the plant, the specific heat was evaluated in each of the simulations. The specific heat is defined according to Equation (3.1), and is a measure of how large energy input is needed in the stripper for a certain amount of purified CO$_2$.

$$\text{Specific heat(MJ/kg CO}_2\text{)} = \frac{\text{Reboiler duty}}{\text{Mass flow of CO}_2\text{ in stripper top product}} \tag{3.1}$$

## 3.5 Economic evaluation

A total of eight designs were evaluated based on process economics. For the six designs of Part 1 (refinery case and steel mill case, at three different sizes each), the CAPEX were estimated using the method described in Section 3.5.1. The results of the CAPEX estimation for the steel mill case was then utilized to estimate the cost of the two designs in Part 2 (seasonally varying versus constant load). OPEX

was estimated for all eight designs according to Section 3.5.2. For the two designs in Part 2, a sensitivity analysis was carried out to investigate the impact of different economic parameters, as described in Section 3.5.3

The economic performance of the designs was assessed by the annualized avoidance cost, which is calculated by adding the OPEX to the annualized CAPEX, and dividing by the annual rate of $CO_2$ avoided as shown in Equation (3.2).

$$\text{Specific cost}(€/\text{tonne } CO_2 \text{ avoided}) = \frac{\text{Annualized CAPEX + OPEX}}{CO_2 \text{ avoided}} \tag{3.2}$$

### 3.5.1 CAPEX estimation

Table 3.4 summarizes the assumptions for the CAPEX estimation. An early stage CAPEX screening such as the one performed in this work usually has an uncertainty of ±30-50% [54]. The CAPEX estimation was performed via different methods for the $CO_2$ separation plant (cf. Figure 3.7), and the liquefaction plant (cf. Figure 2.3). For the separation plant, each piece of equipment was evaluated individually. The equipment taken into account for the separation plant is described in Appendix B. An initial equipment cost estimation was performed using cost estimation data published in peer-reviewed literature predominantly based on Aspen PLUS cost data [31], [55], [56]. The equipment installed cost (EIC) for each piece of equipment (taking into account such costs as engineering, piping etc.) and the total installed cost (TIC) of the separation plant was then estimated according to the methodology of a study by Ali et al. published in 2019 [57], describing a cost estimation strategy for absorption based post-combustion $CO_2$ capture. In the study by Ali et al., the enhanced detailed factor (EDF) is used in which each piece of equipment is treated as an individual plant, which ultimately results in a more accurate, early-stage cost estimation compared to other methods [57]. The CAPEX estimation of the separation plant is further described in Section 3.5.1.1. The TIC of the compression sequence and liquefaction plant was evaluated as one unit, using an article by Deng et al. specifically treating liquefaction of $CO_2$ [34] as further described in Section 3.5.1.2.

**Table 3.4:** Cost estimation assumptions.

| | |
|---|---|
| Plant life time | 25 years (2 years construction, and 23 years operation) |
| Cost year | 2016 |
| Discount rate | 7.5 % |
| First-of-a-kind or N:th-of-a-kind | N:th-of-a-kind |
| Greenfield or brownfield | Brownfield |
| Location | Rotterdam (Location factor 1) |
| Currency conversion factor (€ to NOK 2016) | 9.7 NOK/€ |
| Material flue gas fan | CS ($f_{mat}$ 1) |
| Material pumps | SS316 Machine ($f_{mat}$ 1.3) |
| Material other equipment | SS316 Welded ($f_{mat}$ 1.75) |

The CAPEX estimation was finalized adding the TIC of the separation and liquefaction plant toghether (Equation (3.3)). As described in the paper by Ali et al., the annualized CAPEX can be calculated using an annualized factor, r [57]. The annualized factor was calculated using the plant operational lifetime n of 23 years, and the discount rate p of 7.5%, according to Equation (3.4) [57]. The annualized CAPEX was then calculated according to Equation (3.5).

$$\text{TIC} = \text{TIC}_{\text{liquefaction plant}} + \text{TIC}_{\text{separation plant}} \tag{3.3}$$

$$r = \sum_{n=1}^{n} \left[ \frac{1}{(1+p)^n} \right] \tag{3.4}$$

$$\text{Annualized CAPEX} = \frac{\text{TIC}}{r} \tag{3.5}$$

#### 3.5.1.1 TIC, separation plant

Figure 3.9 shows an overview of the methodology used to estimate the TIC of the separation plant. The equipment cost of the separation plant was based on equipment specific sizing parameters (Table 3.5), and existing cost estimation data collected from literature [31], [55], [56], which was used to set up cost power functions for each specific type of equipment according to Equation (3.6). The cost power functions and the calculation procedure are further described in Appendix B.

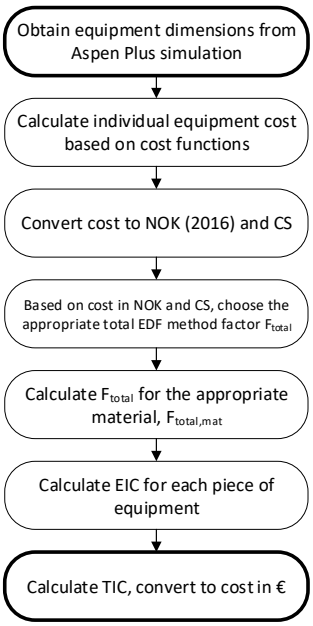


**Figure 3.9:** Summary of the methodology used to estimate the cost of the separation plant.

**Table 3.5:** Sizing parameters of the equipment.

| Equipment | Sizing parameter | Unit |
|---|---|---|
| Column and tank | Volume | $m^3$ |
| Heat exchanger | Area | $m^2$ |
| Pump and fan | Work | kW |
| Reclaimer | Mass flow HSS | kg/h |

Sizing parameters for the design to be evaluated were obtained from Aspen Plus, and from the cost functions, the cost of each piece of equipment was determined. The equipment cost was then converted to the desired costing year (2016) prices using the chemical engineering plant cost index (CEPCI).

$$\text{Cost} = C_0 \cdot (\text{sizing parameter})^n \tag{3.6}$$

Hereafter, a summary of the costing methodology described by Ali et al. is presented. The method is described in more detail in the paper by Ali et al. [57]. To utilize the data of the paper, the equipment cost of each piece of equipment had to be converted to the respective cost for carbon steel (CS) and in Norwegian Kroner (NOK), as shown in Equation (3.7). The conversion to carbon steel was perfomed using a material factor specified for each type of equipment, as shown in Table 3.4. The exchange rate of the costing year of interest (2016) was assumed to be 9.7 NOK/€.

$$\text{Cost(NOK,CS)} = \text{Cost(€,mat)} \cdot f_{material} \cdot \text{exchange rate} \tag{3.7}$$

To estimate the EIC for each piece of equipment the enhanced detailed factors were used. The factors are divided into five main categories. The first four; direct costs, engineering costs, administration costs, and commissioning costs constitute so called known costs. The final factor takes into account contingency. What values of the factors to use is based on the cost of the specific piece of equipment in NOK and CS, as shown in Appendix B, where a detailed break down of the factors are also shown. For each cost interval, a total cost factor ($F_{total}$) was obtained by adding all factors together, as shown in Equation (3.8).

$$F_{total} = f_{direct} + f_{eng} + f_{adm} + f_{com} + f_{cont} \tag{3.8}$$

If the cost was to be obtained in a different material than CS, ($F_{total}$) was corrected using the material factor, as shown in Equation (3.9). In this equation, $f_{equip}$ is the equipment factor, which is equal to one for all cases, and $f_{piping}$ is the piping factor, one of the direct cost factors.

$$F_{total,mat} = F_{total} + (f_{material} - 1)(f_{equip} + f_{piping}) \tag{3.9}$$

EIC for each piece of equipment was then obtained by multiplying $F_{tot,mat}$ with the equipment cost obtained from the power-law cost functions (Appendix B) as shown in Equation (3.10).

$$\text{EIC} = \text{Equipment cost} \cdot F_{total} \tag{3.10}$$

TIC was calculated by summing the costs of each individual piece of equipment, as shown in Equation (3.11). The cost of the amount of MEA required to start the plant was also added, based on an assumed total circulation time of the solvent of 40 min adopted from [58]. Finally, the cost was converted back to euro 2016 prices.

$$\text{TIC}_{\text{separation plant}} = \sum \text{EIC} + \text{MEA start cost} \tag{3.11}$$

#### 3.5.1.2 CAPEX, compression and liquefaction plant

Since the liquefaction plant was not fully modeled in Aspen, sizing parameters for individual pieces of equipment was not available. The liquefaction plant was evaluated as a single unit, using the $CO_2$ flow into the compressors as sizing parameter. The equipment cost C was calculated using using the power law and an escalation factor exponent of 0.6, as shown in Equation (3.12). In the equation, $C_0$ and $CO_2$ flow $\text{rate}_0$ is the cost (25.5 M€) and flow rate (37.31 $\text{kgCO}_2/\text{s}$) for a plant with the same delivery and liquefaction pressure as assumed in this work (7 bar and 20 bar respectively), obtained from the paper by Deng et al. [34].

$$C = C_0 \left( \frac{\text{CO}_2 \text{ flow rate}}{\text{CO}_2 \text{ flow rate}_0} \right)^{0.6} \tag{3.12}$$

To calculate the TIC of the liquefaction plant, the equipment cost was multiplied with factors taking into account process contingency (15%), project contigency (20%), owner cost (7%) and indirect cost (14%) as shown in Equation (3.13).

$$\text{TIC}_{\text{liquefaction plant}} = C \cdot f_{proj.cont} \cdot f_{proc.cont} \cdot f_{ind} \cdot f_{own} \tag{3.13}$$

It should be noted that the compression sequence utilized in the work by Deng et al. contains 3 compressors, and not 2 as in this work. This naturally results in an overestimation of CAPEX for the liquefaction plant in this thesis. However, in the work by Deng et al., the equipment cost of a compression train with 3 or 4 compressors displayed a surprisingly small difference, which is why the estimation in this work was deemed good enough. There will also be an overestimation of the liquefaction plant OPEX, since the energy and cooling demand of the entire liquefaction plant was based on the energy demand of the compression sequence, and a 2 stage compression train results in a higher energy demand than a 3 stage compression train.

### 3.5.2 Operational Expenditures

The operating hours of the capture plant were assumed the same as the average amount of operating hours as for the industrial plant in question. For a typical refinery, it is 8322 h/year, and for a typical steel plant, 7972 h/year [25]. To account for the downtime of the plants, the plants were assumed to undergo maintenance periods during the end of the summer, for 438 and 788 hours respectively. The annualized fixed OPEX included maintenance, insurance and labor and was assumed to be 6% of the TIC [34].

The electricity price was evaluated for every operating hour, and was based on a moving average of the Swedish 2019 spot prices of Nord Pool [59]. Since only seasonal variations are of interest, a moving average window of 720 h, corresponding to a month, was deemed reasonable. For the simulations in Part 1, where CCS was prioritized over DH, the lost revenue of DH was taken into account. The DH prices was estimated based on a relation between electricity price and DH price, in accordance with marginal heat generation cost modeled for the district heating system of Gothenburg following the methodology by Romanchenko et al. [60]. Thus, the DH price was also estimated for every operating hour. The electricity price and DH price are displayed in Figure 3.10.

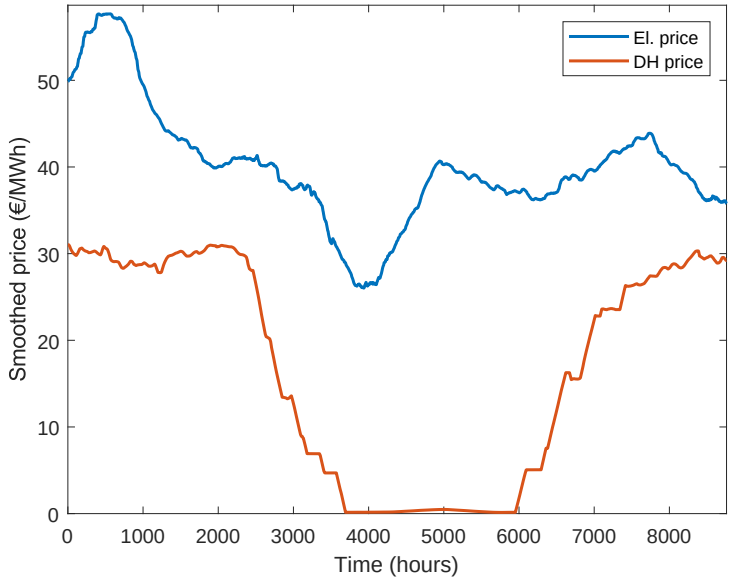


**Figure 3.10:** Electricity price (blue) and DH price (orange), based on Nord Pool spot prices of 2019 in Sweden [59] and marginal heat generation cost according to the method by Romanchenko et al. [60].

For the cooling water, the make-up of MEA (including sludge disposal), the steam used to heat the reboiler and the natural gas, the prices were assumed to not vary seasonally. It was assumed that 1.2 kg make-up of MEA was required per ton of $CO_2$. For the steam price, the cost of the new steam systems needed were taken into account. In the steel mill case, where steam was assumed to be extracted from

the already existing turbines, only extra piping was considered, in accordance with the work by Biermann et al. [31]. For the refinery case, where steam was assumed to be generated by excess heat from process streams, the price included piping as well as extra equipment needed, such as pumps, tanks and heat exchangers, and was based on the work by Ali et al. [14]. The natural gas price was based on the average import price of 2019, however, it was also assumed to be coupled to the average electricity price by a factor of 0.4. For the refinery case designs, NaOH is included in the OPEX since it is needed in the treatment of the DCC purge. The fixed and variable OPEX prices are shown in Table 3.6.

**Table 3.6:** Assumed fixed and variable OPEX prices.

| **Fixed OPEX** | |
|---|---|
| Maintenance, insurance and labor cost | 6% of TIC |
| **Variable OPEX** | |
| Electricity price | Varying |
| Average electricity price | 40 €/MWh |
| DH price | Varying |
| Cooling water price | 0.02 €/m$^3$ |
| MEA price (including sludge disposal) | 2000 €/m$^3$ |
| Steam price, steel mill case | 1 €/t |
| Steam price, refinery case | 3 €/t |
| Natural gas price | 16 €/MWh |
| NaOH price | 270 €/t |

### 3.5.3 Sensitivity analysis

The sensitivity analysis was carried out to investigate the effect of different economic parameters on the specific cost. The first investigated parameter was the absolute CAPEX, which was chosen since the oversized SV plant was assumed to be highly dependent on the estimated CAPEX cost. The second investigated parameter was the average electricity price, to examine the effect on varying energy prices. The average electricity price affects the seasonally varying electricity prices, but it also affects the natural gas price since it is assumed to be coupled to the electricity price. The third investigated factor was the relation between natural gas price and electricity price, which will only affect the natural gas cost, but is interesting to include to be able to investigate the effect of the coupling between energy prices. The parameters were varied one by one by ±50% from their original values.

# 4
# Results and discussion

In the following chapter, the results are presented and discussed. The results from Part 1 and Part 2 are presented and discussed separately, in Section 4.1 and 4.2 respectively. A comparison between the approaches in Part 1 and Part 2, with respect to the economic performance as well as a discussion regarding the implications for the optimal heat integration approach is presented in Section 4.3.

## 4.1 Part 1: Prioritizing EH supply to CCS over DH delivery

In Part 1, six designs of the capture plant, three sizes for the refinery case and the steel mill case respectively, were simulated. Table 4.1 displays the yearly capture rates and and reboiler duties for each design. The yearly capture rates have been calculated using the operational hours as specified in Section 3.5.2. The maximum sizes were used to evaluate the potential for heat integration with the district heating network (Section 4.1.1) as well as the effect on the district heating network (Section 4.1.2). All designs in Part 1 were evaluated economically (Section 4.1.3).

**Table 4.1:** Capture rate and reboiler duty of the capture plants evaluated for the refinery case and the steel mill case in Part 1 of the thesis.

| **Refinery case** | | | |
|---|---|---|---|
| | Minimum | Mean | Maximum |
| Capture rate (kton $CO_2$/year) | 100 | 200 | 306 |
| Reboiler duty (MW) | 12.4 | 24.8 | 38 |
| **Steel mill Case** | | | |
| | Minimum | Mean | Maximum |
| Capture rate (kton $CO_2$/year) | 100 | 565 | 1228 |
| Reboiler duty (MW) | 10.9 | 61.4 | 133.6 |

### 4.1.1 Heat integration of the $CO_2$ separation plant with the district heating network

Table 4.2 displays the cooling demands and temperature levels of the coolers of the $CO_2$ separation plant, for the maximum sizes of the preem and refinery cases (cf. Figure 3.3). The $CO_2$ rich stream exiting the stripper displayed a curved cooling profiled, caused by simultaneous $CO_2$ cooling and condensation of water in the

stream. To better capture the potential heat recovery to the DH network, the cooling demand of the $CO_2$ rich stream was thus distributed over two heat exchangers, the first one cooling to 60°C (4.1) and the second one covering the additional demand, cooling to 20°C (4.2). The division was based on the assumption of a minimum temperature difference of 10°C between the hot streams of the $CO_2$ capture plant and the DH network, and a DH return temperature of 50°C. The largest cooling demand of the capture plant with heat above the required temperature of 60°C is that of the $CO_2$ rich stripper top gas which is condensed and cooled in cooler 4.1. The intermediate coolers of the compression sequence (cooler 5 and 6) also contain heat at a sufficient temperature level, but the amount of heat is small compared to that of the $CO_2$ rich stream. All other coolers have temperatures below 60°C, too low to be utilized for district heating with a minimum temperature difference of 10°C.

**Table 4.2:** Cooling demand of the heat exchangers of the maximum size designs, for the steel mill case and the refinery case.

| | **Refinery** | | **Steel mill** | |
|---|---|---|---|---|
| Cooler | Heat (MW) | Temperature (°C) | Heat (MW) | Temperature (°C) |
| 1. | 26.0 | 50 - 20 | - | - |
| 2. | - | - | 73.4 | 56.6 - 29.7 |
| 3. | 12.5 | 55.8 - 40 | 30.5 | 40.4 - 29 |
| 4.1. | 8.4 | 98.6 - 60 | 22.2 | 92.3 - 60 |
| 4.2 | 2.0 | 60 - 20 | 7.4 | 60 - 20 |
| 5. | 1.0 | 117.2 - 25 | 4.0 | 117.3 - 25 |
| 6. | 1.0 | 125.9 - 25 | 4.3 | 124.7 - 25 |

In Figure 4.1a and 4.1b the respective hot composite curves of the refinery and steel mill cases are displayed (orange). The maximum amount of DH which can theoretically be supplied from the $CO_2$ capture plant (blue), is limited by the minimum temperature difference of 10°C at the pinch. Even though the HCC of the cases are similar, the pinch temperature is different: for the hot streams, at 60°C for the refinery case, 92°C for the steel mill case. This causes the ratio of the theoretical amount of recoverable from the $CO_2$ separation plant to the heat supplied to the reboiler to be much lower in the steel mill case, about 9.7%, while in the refinery case, the amount is 25.5%. The difference in pinch point is caused by the temperature into the stripper reflux condenser (cooler 4.), which for the refinery case is about 99°C, while for the steel mill case only about 92°C.

The difference in temperature has not been extensively investigated in this work, but is likely caused by a combination of different factors. One likely cause is the temperature of the rich solvent stream, which is about 30°C in the steel mill case, and about 46°C in the refinery case. 15% of the $CO_2$ rich stream is introduced to stage 2 in the stripper without being heated (RSS, cf. Section 2.2.1). The temperature difference between stage 2 and stage 3 is much larger in the refinery case than in the steel mill case, possibly caused by the difference in temperature of the $CO_2$ rich stream. The low temperature in the steel mill case may be an effect of

the lower temperature into the absorber of both the flue gas and the lean solvent stream, and by the implementation of ICA, causing lower temperatures in the entire absorber. The concentration of $CO_2$ in the flue gas may also have an effect on the temperature in the stripper, via the rich loading ($CO_2$ to MEA ratio in the rich solvent stream), which is generally higher for higher $CO_2$ concentrations. In the steel mill case, the rich loading is 0.56 while in the refinery case it is 0.51. The rich loading may affect the equilibrium temperature in the stripper, the significance of the difference between the two cases has however not been further investigated.

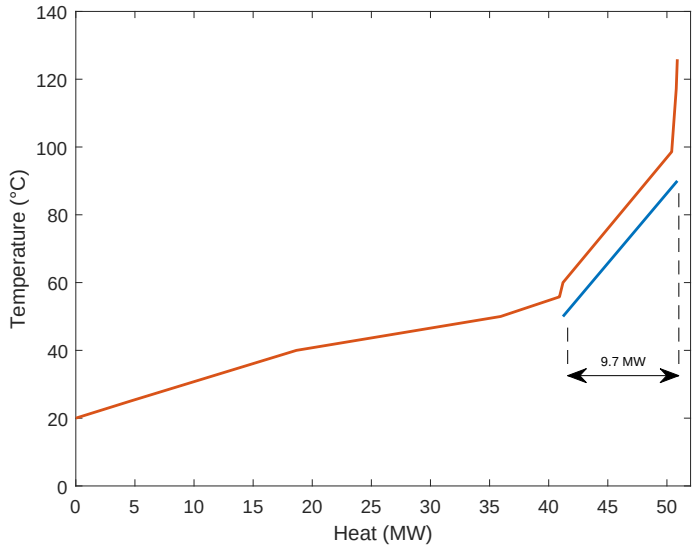


**(a)**

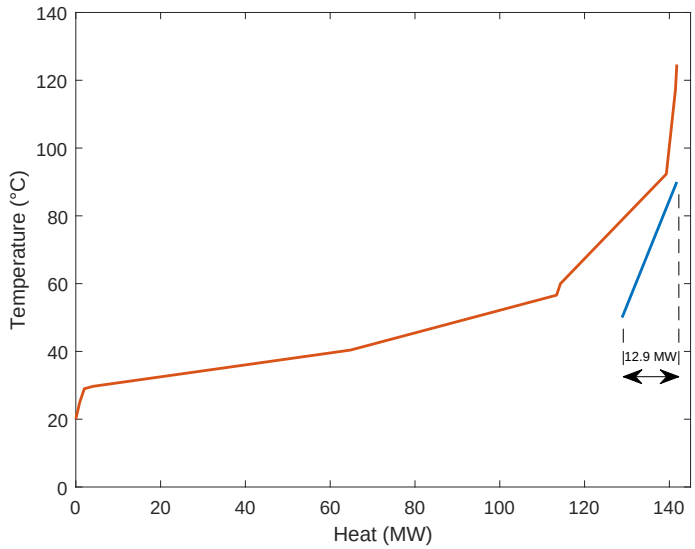


**(b)**

**Figure 4.1:** HCC of the cooling demand of the carbon capture plant (red), and potential heat supply to the DH system (blue), for the refinery case (a) and the steel mill case (b).

It should be noted that the exact amount of recoverable DH is dependent on the chosen minimum temperature difference of 10°C. The dependence in the refinery case is not strong, but it is more pronounced in the steel mill case. For example, a minimum temperature difference of 7°C results in a ratio of recoverable DH to reboiler duty of 26% for the refinery case, and 16% for the steel mill case. Decreasing the minimum temperature level will bring the results of the steel mill case closer to that of the refinery case, however, it will also result in larger heat exchangers. The optimal minimum temperature difference will therefore be a trade-off between the cost of DH loss, and the cost of increased heat exchanger area.

### 4.1.2 Effects of CCS on the district heating network

Due to the difference in the origins of the excess heat (heat collecting system for the refinery case, and CHP for the steel mill case) the DH networks in each industrial case study are affected in differently by the integration with CCS. The low and high temperature DH networks of the refinery case are also affected differently by the heat integration. For the high temperature network, even though 13 MW of heat remained above the lowest temperature (100°C) that could be utilized for district heating, no heat at sufficient temperature to raise the DH water to 140°C remained. Consequently, the entire DH supply in the high temperature network was considered lost. Furthermore, as no heat from the CCS was available at a high enough temperature to supply the high temperature network, it was assumed that all recoverable heat was utilized in the low temperature network. Figure 4.2 shows the heat load of the low temperature network of 2018 (blue line) together with the remaining heat (48 MW), after 11 MW was removed to be utilized for CCS (orange line). The identified recoverable heat from the CCS plant (9.7 MW) was added to the remaining heat in the low temperature network (yellow line), resulting in a total of 57.7 MW. As can be seen from Figure 4.2, during a major part of the year, the remaining 48 MW is enough to cover the DH demand of the low temperature network, while the heat from the CCS plant only becomes useful for some period during winter time.

The total loss of DH in the refinery case during the year was 222 GWh (40% of original supply) without heat recovery from the $CO_2$ separation plant, and 201 GWh with heat recovery (36% of original supply). Of this amount, 200 GWh was lost in the high temperature network, while the rest was lost in the low temperature network. Furthermore, since the DH delivery from Preem refinery to the low temperature network only accounts for about 10% of the DH that GEAB delivers to the local community during normal DH delivery, the total loss is less than 1%, and probably easily compensated with other sources. The heat delivered to the high temperature network, where the greatest loss occurs, may be harder to compensate for.

Figure 4.3 shows the DH supply from the steel mill after extraction to CCS. Only a minor part of the heat (18.8 MW) remains in the system as can be seen from the orange line. With the recoverable heat from the CCS plant, a total of 31.7 MW is available (yellow line). While operating the CCS, the DH demand is only cov-

ered during a limited time in summer. The total yearly loss of district heat supply was calculated to 683 GWh (80% of original supply) without heat recovery fro the $CO_2$ separation plant considered, and 572 GWh (67% of original supply) with heat recovery.

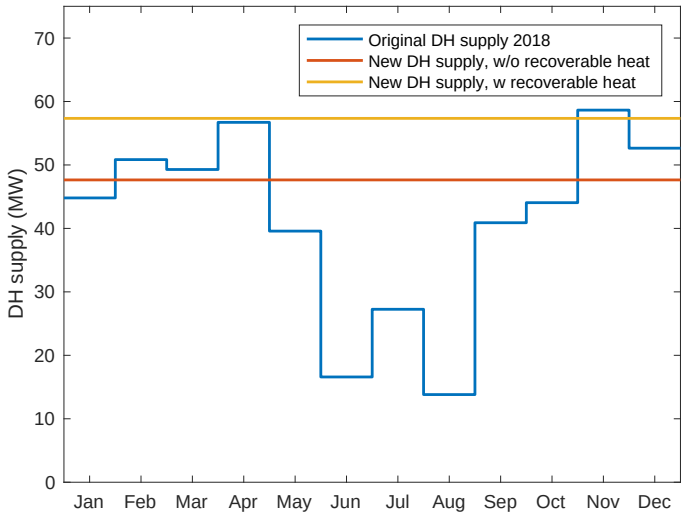


**Figure 4.2:** The low temperature network DH demand of 2018 (blue), together with the available heat after extraction to CCS, with and without the heat recovery potential from the $CO_2$ separation plant (yellow and red respectively).

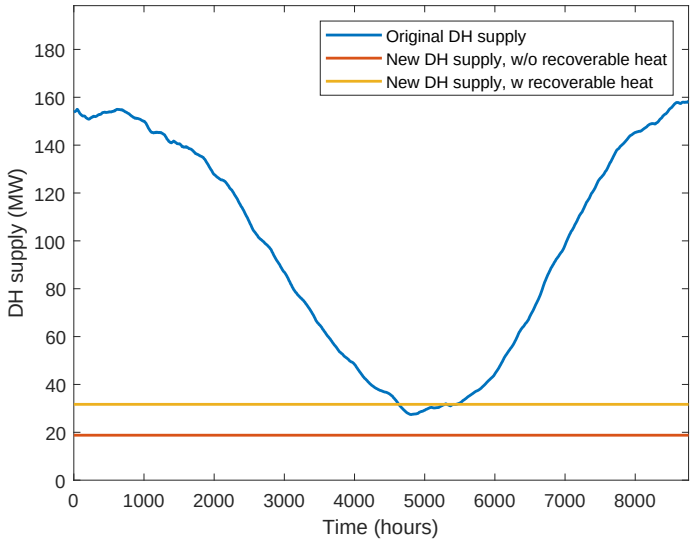


**Figure 4.3:** Original DH supply in the steel mill case (blue), with supply potential after extraction to CCS, with and without heat from CCS plant included (yellow and red respectively).

### 4.1.3 Economic evaluation

Figure 4.4 shows the specific costs of all sizes for the refinery case and the steel mill case, with and without DH revenue loss included. The annualized costs divided into annualized CAPEX, DH revenue loss, and fixed as well as variable OPEX are shown in Figure 4.5. The potential regain of district heat from the $CO_2$ separation plant has not been taken into account. The specific cost when DH revenue loss is taken into account ranges between 40-73 €/tonne $CO_2$, while without DH revenue loss, the specific cost ranges between 24-72 €/tonne $CO_2$. The DH revenue loss causes the annualized cost to increase, especially for the maximum plant sizes. The loss is especially large in the steel mill case maximum size, where most of the heat originally supplied DH is utilized for CCS. The specific cost is also more affected by DH loss for the larger sizes.

If DH revenue loss is not included, the economy of scale is clearly displayed in that the larger separation plants presents smaller specific costs. In the refinery case, the DH revenue loss shows an interesting effect on the specific cost, which is larger for the maximum size than for the mean size. As explained in Section 4.1.2, for the maximum size, all DH revenue from the high temperature network was lost, because no heat at sufficient temperature to supply DH at 140°C remained. This was not the case for the mean and minimum sizes, where it was assumed that utilizing heat from the low temperature network is preferred, since it was less affected by the heat integration. Thus, as little heat as possible was extracted from the high temperature network. For example, for the mean size, the reboiler duty was 24.8 MW. Consequently, only 13.8 MW from the high temperature network was utilized, thus, 13.2 MW of heat at a temperature of at least 130°C remained in the system. Additionally, between the temperatures of 100°C and 130°C, 13 MW remains, as shown in the grand composite curve in Appendix A. Consequently, part of the 13 MW of heat below 130°C remaining in the network can be utilized to heat the DH water between 90°C and 120°C, and the 13.2 MW of high temperature heat can be used primarily to raise the DH water from 120°C to 140°C. The low specific cost of the mean and minimum sizes is thus an effect of that a large amount of heat in the high temperature network is retained.

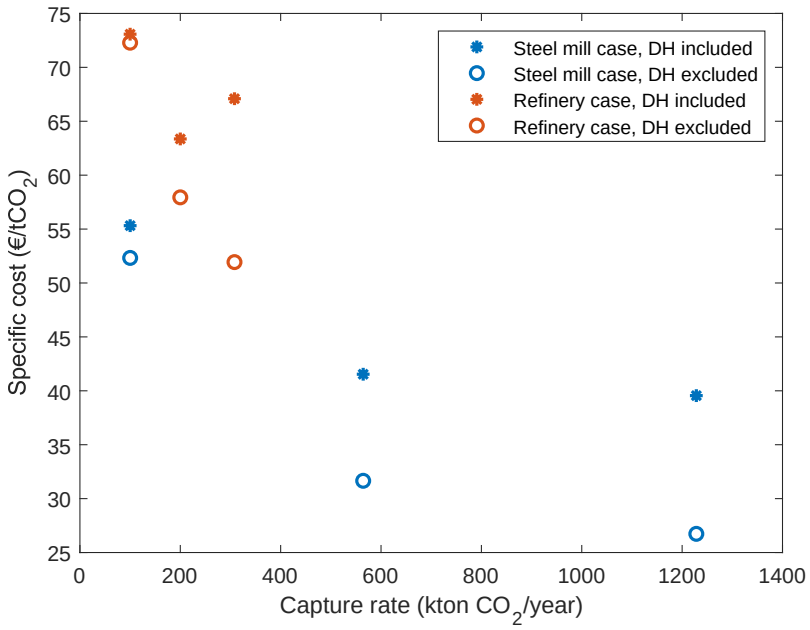


**Figure 4.4:** Comparison of specific cost between refinery case and steel mill case, with loss of DH revenue included or excluded.

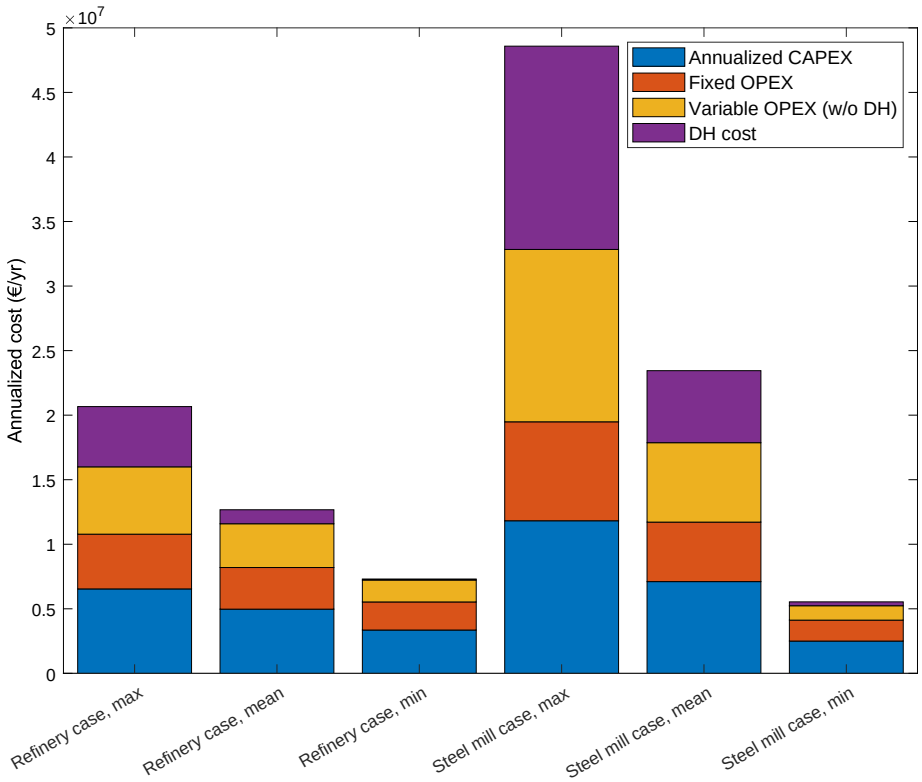


**Figure 4.5:** Comparison of costs between refinery case and steel mill case, all sizes. The purple bars represent the loss of DH revenue (denoted DH cost for simplicity).

### 4.1.4 Part 1, implications of the results

The results of the two case studies imply that opportunities for extraction of district heat from the $CO_2$ separation plant exist, especially via the stripper reflux condenser, but that the potential is very case dependent, and affected both by the properties of the flue gas, such as concentration and temperature, and the district heating network. The minimum temperature difference also has an effect on the specific amount of DH recovery. The effect of the flue gas properties is clearly seen from it's effect on the stripper reflux condenser temperature, which shows to have a significant impact on the amount of heat that can be extracted from the $CO_2$ separation plant. The effect of the characteristics of the excess heat and the district heating network was most clearly displayed in the refinery case. The size of the plant was limited by the availability of heat at a sufficient temperature, and it was not possible to replace the heat in the high temperature network.

To summarize, to effectively integrate a $CO_2$ separation plant with an industry and the district heating network, a detailed case study and economic optimization would be required for the plant of interest, investigating for example modifications to the design of the $CO_2$ separation plant to improve heat recovery. In particular, there are implications that efforts to raise the temperature in the stripper reflux condenser may be interesting. Whether such modifications are possible without causing for example high reboiler duties, however, has to be further investigated. There may also be other heat sources related to the capture plant, such as the hot flue gases, which are cooled in the DCC. Potentially, the temperature of the stripper reflux stream could also be raised with heat pumps. Such investigations are motivated by the economic evaluation, which shows that that DH revenue loss may be costly, even at scales comparable to the CAPEX and OPEX of the capture plant. However, the actual effect of the recoverable amount of DH from the $CO_2$ separation plant on the district heating network should also be taken into account. For example, in the refinery case, even though 25.5% of the heat supplied to the reboiler could be recovered from the $CO_2$ capture plant, only a small amount of this heat proved to actually have an application, and only during a limited time of the year. In such a case, extraction of DH from the separation plant may not be economically beneficial. In this case it may have proven profitable to invest in a heat pump, so that heat could also be recovered to the high temperature DH network.

The importance of the DH delivery of the specific source also has to be considered. In the refinery case, the DH delivery to the low temperature network only accounts for about 10% of the total DH delivery from GEAB to the local community, which means that even if more had been lost, the heat may have been replaceable with other sources. In the steel mill case, the heat provided from the CHP is the main source of DH in the local community, meaning that the DH would be harder to replace. The environmental impact of having to implement other sources of heat then has to be considered. Losing about 80% of DH delivery in the steel mill case could potentially result in about 163 kton $CO_2$ equivalents of additional emissions each year. Compared to the 1228 kton $CO_2$ reduction if CCS is implemented, implementing CCS is clearly more beneficial to the climate.

## 4.2 Part 2: Prioritizing retained DH supply over capturing as much $CO_2$ as possible

In Figure 4.6a, the SV heat availability curve (blue) as well as SV reboiler duty (orange) is presented. For most of the year, it is possible to operate the reboiler at the same duty as the amount of heat available, i.e. the heat that is not utilized for DH. However, as is shown in the figure, for some hours during winter time there is a heat deficit that needs to be compensated for to be able to operate the reboiler at the minimum heat level.

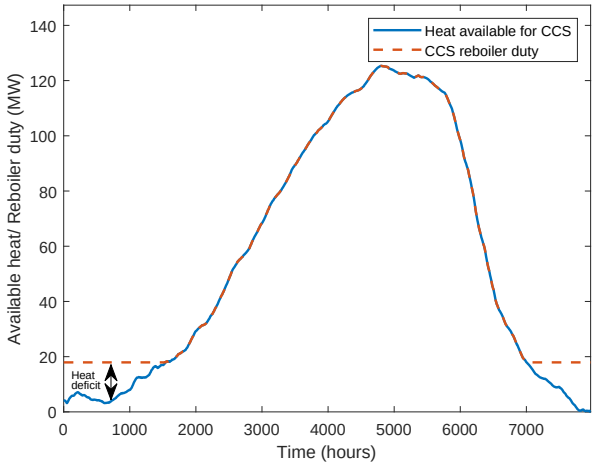


**(a)**

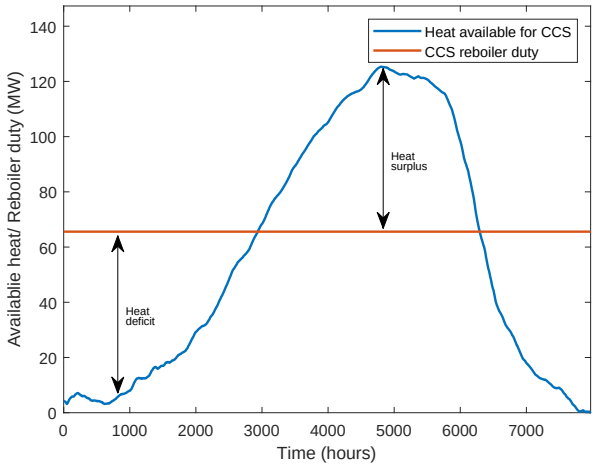


**(b)**

**Figure 4.6:** Comparison of heat availability curve (blue) and reboiler duty (orange) for the SV plant (a) and the CL plant (b). The heat deficit during winter is pointed out for both plants, corresponding to when the blue curve is below the orange one. For the CL plant, the heat surplus during summer time is pointed out as well.

The plant for the CL operational mode had a constant reboiler duty of 65.5 MW, which is displayed in Figure 4.6b in relation to the heat availability curve. During winter time, there is a heat deficit, while during summer, there is a heat surplus, i.e. the amount of available heat is larger than the amount of heat required for the capture plant reboiler. Thus, during summer, additional cooling will still be required for the steel mill CHP plant, however not as much as compared to the original situation without CCS integration. The potential amount of recoverable heat from the CL capture plant to DH was estimated in a similar way as for the maximum sizes of Part 1, and it was concluded that the heat recovery potential was 6.3 MW. The recoverable heat was however not taken into account in the design of the plant, which would be necessary to optimize the heat integration between the capture plant, DH supply and industrial plant and to minimize the amount of natural gas needed. Both capture plants were designed to achieve the same yearly amount of $CO_2$ avoided, and Table 4.3 shows a comparison of the performance of the plants. The plants are evaluated based on the average amount of operating hours for a steel mill, i.e. 7972 hours/year.

**Table 4.3:** Capture plant performance of SV plant and CL plant.

| | **SV** | **CL** |
|---|---|---|
| (Design) reboiler duty (MW) | 125.3 | 65.6 |
| Capture rate (kton/year) | 567.3 | 602.9 |
| $CO_2$ avoided (kton/year) | 562.4 | 562.4 |
| Extra emissions from natural gas (kton/year) | 4.9 | 40.5 |
| Energy input, EH (GWh/year) | 452.6 | 320.0 |
| Energy input, natural gas (GWh/year) | 24.7 | 202.8 |
| Non-utilized EH (GWh/year) | 0 | 132.6 |

In Figure 4.7a and 4.7b, the hourly $CO_2$ capture rate is presented of the SV plant and CL plant respectively. The total area (blue + orange) represents the the total amount of annually captured $CO_2$. Due to the heat deficit during some periods, extra emissions from combustion of natural gas were taken into account. These emissions are represented by the orange fields, while the blue field represents the $CO_2$ avoided. During summer time when there is no heat deficit, all captured $CO_2$ is also avoided, while during winter, the $CO_2$ avoided is less than the total amount of captured $CO_2$. At the design reboiler duty for the SV plant, the capture rate was 144 tonne $CO_2$/hour. The design capture rate corresponds to a 90% separation rate in the absorber and a 84% capture of the total BFG $CO_2$ content. The hourly capture rate for the CL plant was 75.6 tonne $CO_2$/hour, a 44% capture of the BFG $CO_2$ content. The $CO_2$ avoided corresponds to capturing about 41% of the BFG $CO_2$ content, and 17% of the total direct emissions of the steel mill plant. For the SV plant, the share of $CO_2$ avoided to total amount of captured $CO_2$ was 99% (i.e. blue area divided by total area in Figure 4.7a). For the CL plant, the corresponding share was 93% (blue area divided by total area in Figure 4.7b).

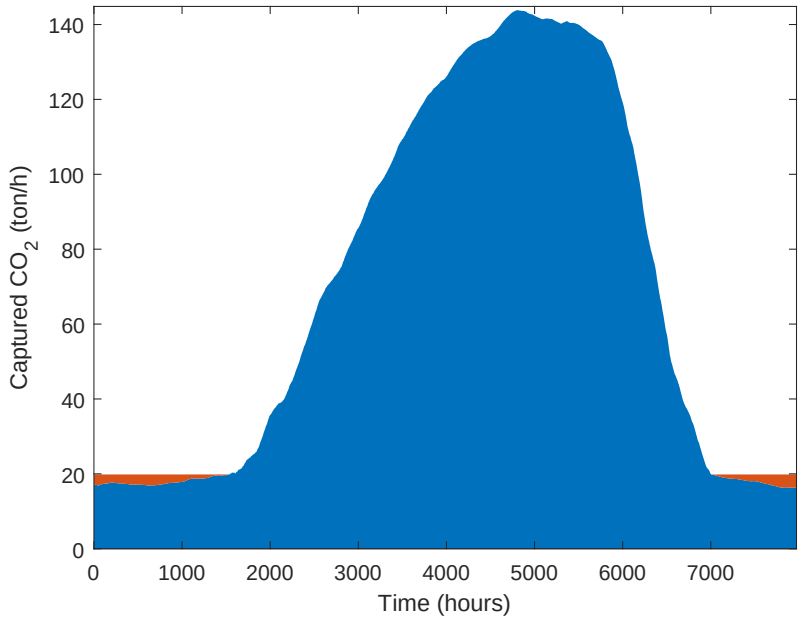


**(a)**

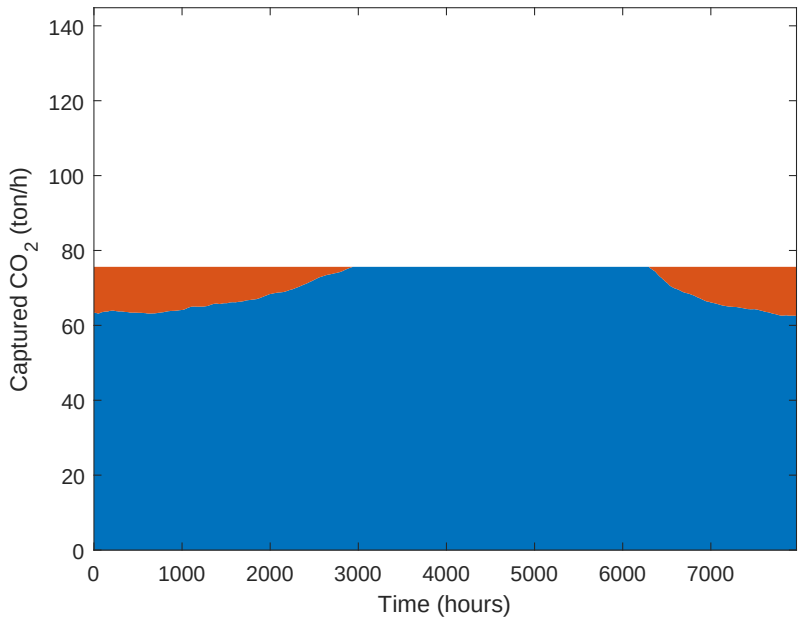


**(b)**

**Figure 4.7:** Hourly capture rate of $CO_2$ for the SV plant (a) and CL plant (b). The total area (blue + orange) represents the the total amount of annually captured $CO_2$. The orange area represents natural gas emissions. The blue area represents $CO_2$ avoided, and are thus of equal size in both figures.

In Figure 4.8, the specific heat is plotted against the absorber separation rate for the off-design simulations of the SV plant. As can be seen, the specific heat is at is lowest for a separation rate of about 35%. For even lower separation rates, the specific heat increases significantly. A probable cause for this is that the separation efficiency decreases due to poor wetting. To have an even lower reboiler duty than the one chosen for the minimum heat level would thus probably increase the specific heat even more, and would not contribute a lot to the total capture of the SV operation. To shut down the plant entirely during winter would eliminate the need for natural gas combustion. However, as was seen in Figure 4.7a, since the total amount of captured $CO_2$ during winter is mostly also avoided, to operate the plant at a minimum heat level with natural gas compensation will still be favorable in terms of total $CO_2$ avoidance. Hence, it can be concluded that even though the minimum heat level was chosen based on convergence issues rather than a physical limitation of the process, to operate the plant at an even lower minimum level, or to shut down the plant, would not automatically gain the overall performance of the plant.

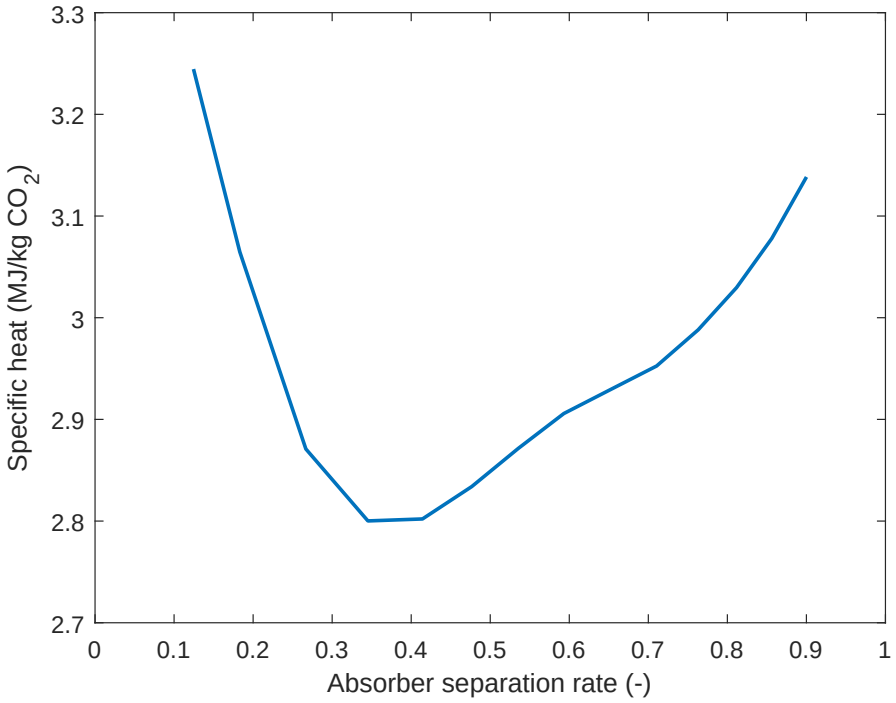


**Figure 4.8:** Specific reboiler duty as function of the absorber separation rate for the off-design simulations.

### 4.2.1 Economic evaluation and sensitivity analysis of SV plant and CL plant

The CAPEX of the SV plant and CL plant were estimated using the fitted cost curve obtained in Part 1. The calculated CAPEX for the plants are presented in Appendix C. The results from the total economic evaluation of the SV plant and the CL plant is presented in Figure 4.9, divided in to annualized CAPEX, fixed OPEX and variable OPEX. The specific cost is also displayed as the pink dots. In Figure 4.10, only the variable OPEX of the SV and CL plant are displayed. The OPEX is divided into its different parameters, i.e. cost of electricity, natural gas, MEA, steam and cooling water.

As can be seen in Figure 4.9, the annualized CAPEX and fixed OPEX are smaller for the CL plant, since those economic parameters are determined by the design of the plant. The variable OPEX is on the other hand larger for the CL plant than for the SV plant. The reason for this is shown Figure 4.10, where it is seen that the natural gas cost constitutes a significant part of the variable OPEX of the CL plant, causing the total cost of variable OPEX to be higher than for the SV plant. The total annualized cost for the CL plant is however smaller than for the SV plant, resulting in a somewhat smaller specific cost as well. Comparing the relation between the cost of annualized CAPEX, fixed OPEX and variable OPEX of both plants, it is evident that the SV plant is oversized in relation to the operation of the plant. Despite the oversized plant, however, the specific cost of the plant is still comparable to the one for the CL plant.

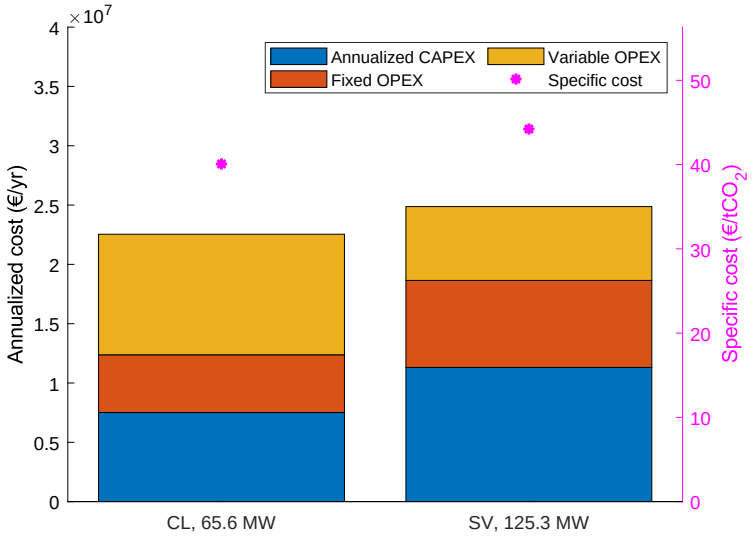


**Figure 4.9:** Economical comparison between the SV plant and the CL plant. The left y-axis shows annualized cost, while the right y-axis shows specific cost. The annualized cost is divided into annualized CAPEX (blue), fixed OPEX (orange) and variable OPEX (yellow).

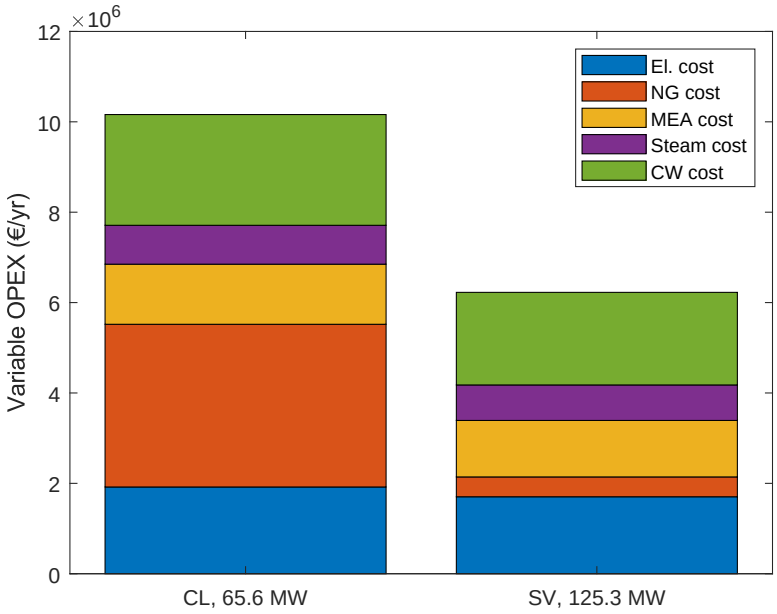


**Figure 4.10:** Economical comparison of the variable OPEX between the SV plant and the CL plant. The OPEX parameters taken into account are electricity (blue), natural gas (orange), MEA (yellow), steam (purple) and cooling water (green).

In the sensitivity analysis, different economic parameters were varied to investigate the effect on the specific cost. The values of the varied parameters are presented in Table 4.4, and the impact on specific cost is presented in Figure 4.11. The relation between natural gas price and electricity price is for simplicity denoted ”NG price”, since that is the only price that is affected.

As can be seen in Figure 4.11, the change in absolute CAPEX had the greatest impact on the specific cost for both plants. However, as expected, the SV plant was more sensitive to the change compared to the CL plant, since the CAPEX constitutes a larger part of the annualized cost of the SV plant. Both average electricity price and NG price had a greater impact on the CL plant specific cost than on the specific cost of the SV plant. For the NG price, this is expected, since the natural gas cost constitutes a very small part of the SV variable OPEX, while it is the largest part of the CL variable OPEX. Considering that the average electricity price affects both the electricity cost and the natural gas cost, it is reasonable for that parameter to have a greater impact on the CL plant as well.

The specific cost of the CL plant is almost consequently lower than that of the SV plant. The exception is seen for lowering the absolute CAPEX by -50%, where the SV plant is seen to become more favorable than the CL plant. Considering the other two investigated parameters, the SV plant is seen to be fairly robust, especially regarding change in NG price, but also the change in average electricity price does not affect the specific cost significantly. By extrapolating the dotted lines as well as the full lines, it was seen that the intersection between the SV plant specific

cost and CL plant specific cost occurs around a 70% increase in average electricity price and NG price respectively. Thus, it can be concluded that for a scenario with a high increase in energy prices, the SV plant would be favorable.

**Table 4.4:** Values of the varied parameters in the sensitivity analysis, for -50%, 0 and +50% change.

| Parameter | -50% | 0 | +50% |
|---|---|---|---|
| Absolute CAPEX (M€), SV | 61.1 | 122.2 | 183.3 |
| Absolute CAPEX (M€), CL | 40.6 | 81.1 | 121.7 |
| Average electricity price (€/MWh) | 20 | 40 | 60 |
| NG price (€/MWh) | 8 | 16 | 24 |

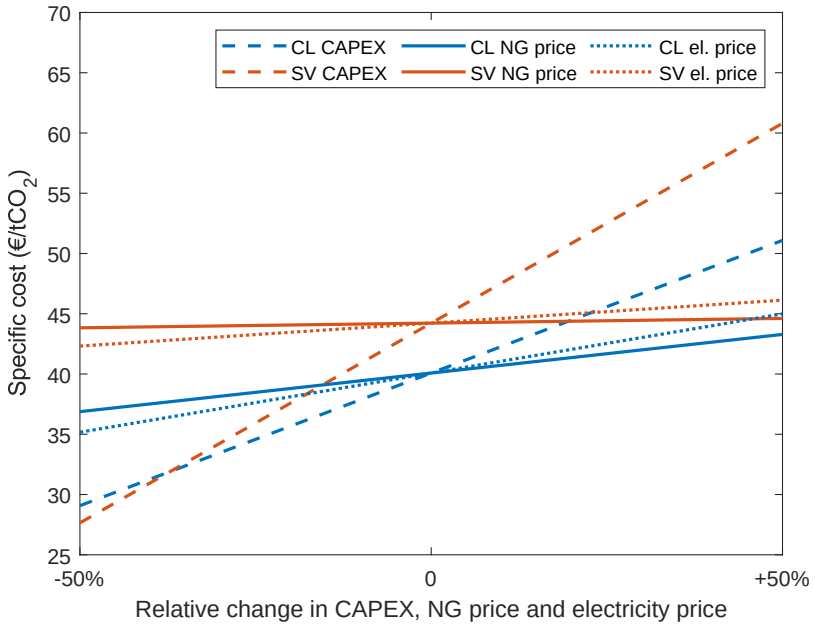


**Figure 4.11:** Sensitivity analysis for the SV plant (orange) and the CL plant (blue). The y-axis displays specific cost, while the x-axis represents relative change of CAPEX, NG price and average electricity price. The lines represents change in specific cost due to change in one of the parameters included in the sensitivity analysis. Dashed lines represents CAPEX, full lines represents NG price and dotted lines represents average electricity price. Note that the y-axis does not start from zero.

### 4.2.2 Part 2, implications of the results and discussion of optimization

The economic evaluation and comparison between the steel mill capture plants of Part 2 showed that the SV plant and the CL plant are comparable, with specific costs of about 40-45 €/t $CO_2$ avoided. The plants are, however, in no way optimized, but are merely set to the extreme values of operating the capture plant while retaining

district heating delivery. An optimum might exist, both in size and in operation of the plant, that yields a plant with lower specific cost. Moreover, the optimal plant should be a plant that is robust to changes in parameters that influences size, operation and economics. Table 4.5 shows the parameters influencing the SV and CL plants. The influence of the energy prices and the CAPEX were investigated in the sensitivity analysis. The results are indicated in the table, where L stands for low sensitivity, I for intermediate sensitivity and H for high sensitivity. The other three parameters, i.e. DH supply peak load, length of seasons and size of heat deficit, were not investigated, but should be considered in the optimization.

**Table 4.5:** Parameters to consider in design and operation. L, I and H stands for low, intermediate and high sensitivity respectively.

| | **SV** | **CL** |
|---|---|---|
| Energy prices | L | H |
| CAPEX | H | I |
| DH supply peak load | - | - |
| Length of seasons | - | - |
| Size of heat deficit | - | - |

The sensitivity analysis showed that the estimated energy prices have an influence on the specific cost of the plants. The CL plant was however seen to be more sensitive towards changes in energy prices, while the SV plant was fairly robust regarding those parameters. Furthermore, the sensitivity analysis also showed that regardless of the operation of the plant, a change in estimated CAPEX had the greatest effect on the specific cost of the three investigated parameters. The SV plant was however even more sensitive, implying that the estimated CAPEX will be an even more important factor to consider when designing a plant that is oversized in relation to its operation. One option to consider might be to size the plant for the peak load, as for the SV plant, but to choose a higher minimum level of heat to operate on during winter. Such plant would be more robust to CAPEX changes than the SV plant, since it would be less oversized in relation to its operation. However, a larger heat deficit would need to be compensated for, implying a higher sensitivity to changing energy prices. Another option could be to size the plant for a somewhat smaller peak load than for the SV plant, but to still operate it in a seasonally varying manner. Similar to the SV plant, such plant would be more robust to changes in energy prices than the CL plant. It would also generate a lower annualized cost than the SV plant, since the CAPEX would decrease. However, also the amount of $CO_2$ avoided would decrease, thus, it is difficult to tell whether the specific cost would increase or decrease.

The district heating supply curve determines both the size operation of the plants, thus, the shape of the supply curve has a great impact of the performance of the capture plants. The size of the peak load of the heat availability curve will determine the maximum possible size of the CCS plant. The operation of the plant will be affected by the width of the curve, i.e. by the length of the periods at different heat levels. If, for example, there would be a longer summer period, the CCS plant would be able to operate at a higher capacity for a longer period of time, which would be

favorable for the total capture of the plant. Thus, to fully evaluate the performance of these capture plants, it would be necessary to investigate the operation over a longer period of time than one specific year. Furthermore, the curve of available heat will determine the size of the potential heat deficit, and thus determines the amount of natural gas needed for heat supply compensation. For a plant with large need for natural gas, such as the CL plant, the amount of natural gas needed has shown to have an important impact on both specific cost and amount of $CO_2$ avoided for the plant.

To fully evaluate and optimize a capture plant operating on EH that is currently utilized for DH, a detailed investigation of the influence of all the aforementioned factors needs to be carried out. A generic curve of available heat, not only based on one year, should be investigated, and the influence of variations to the curve. The future sensitivity in energy prices should also be examined.

## 4.3 Economic comparison of steel mill capture plants of Part 1 and Part 2

Figure 4.12a shows annualized cost and specific cost for all evaluated CCS designs regarding the steel mill plant. The bars denoted (1) corresponds to the designs from Part 1 of the thesis, while the ones denoted (2) are from Part 2 of the thesis. The minimum size from Part 1, with a reboiler duty of only 10.9 MW, has, as expected, the lowest absolute cost but the highest specific cost due to its low capture rate. The other four plants are all quite similar with respect to specific cost, meaning that by only considering the specific cost, one of these plants can not be deemed more feasible than the others. The plants most alike among the five are the mean size plant from Part 1 and the CL plant from Part 2. The designs are quite similar, resulting in almost equal CAPEX costs and fixed OPEX costs. However, also the variable OPEX costs are similar, which is not evident in beforehand since the OPEX evaluation differs a bit between those plants, with one taking DH cost into account, and the other taking cost of natural gas into account. Furthermore, the two plants are comparable in $CO_2$ avoidance (cf. Table 4.1 and 4.3), making their specific costs similar as well.

To estimate the impact of the DH revenue loss on the specific cost, the DH cost was removed from the annualized costs of the plants in Part 1. Figure 4.12b again shows the comparison between the plants in Part 1 and Part 2, but with the DH cost removed. Considering specific cost, the maximum size from Part 1 is clearly superior in being the most economically feasible. The mean size from Part 1 also becomes superior to the CL plant from Part 2, since the DH cost has been removed but the natural gas cost remains. As was concluded in Section 4.1.3, the loss of DH revenue has a great impact on the economic results for the plants where CCS is prioritized over DH supply, especially in the maximum size plant.

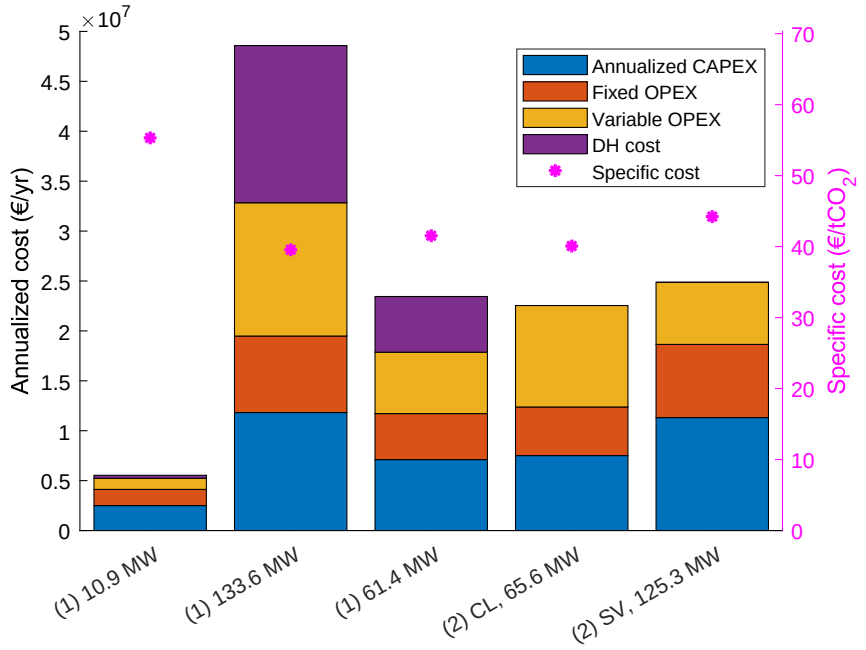


**(a)**

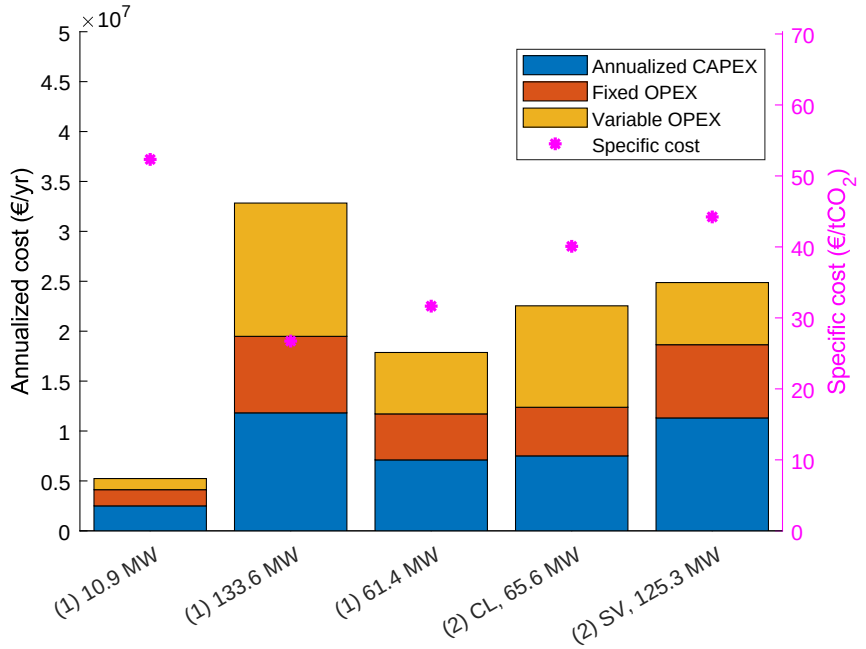


**(b)**

**Figure 4.12:** Annualized cost (left y-axis) and specific cost (right y-axis) for all evaluated CCS sizes regarding the steel mill plant. The bars denoted (1) corresponds to the sizes from Part 1 of the thesis, while the ones denoted (2) are from Part 2 of the thesis. The design reboiler duty of the capture plants are specified on the x-axis. In (a), the lost revenue of DH is included (denoted DH cost), while in (b), it is excluded.

### 4.3.1 Heat integration, influence on the preferred approach

To choose the best integration option, design and operational mode for a CCS plant when a DH network is involved is in essence a question on how DH and CCS is valued. In Part 1, CCS was prioritized over DH, while in Part 2, DH was prioritized. As the situation is today, DH is highly valued, and is seen as an efficient way to utilize EH. Loss of DH delivery also proved very expensive in the economic evaluation, causing the annualized cost to become significantly larger for Part 1, and the integration option of Part 2, in the current situation, is the more viable option. CCS is not highly valued, and the implementation in industry has not been extensive. However, as CCS may be a necessary addition in industry to reach the current climate goals, CCS may have to be valued differently in the future. If CCS is necessary to reach the climate goals, perhaps it should be valued as highly as cleaning the flue gas from other harmful compounds.

How CCS is valued also leads back to the definition of EH in this work. If CCS is in fact considered a necessary addition to an industrial plant, then heat that could potentially be utilized for CCS should perhaps not be considered EH at all, but rather an internal heat integration potential to the industrial plant. In that case, heat discharged from industrial processes, which could be utilized for CCS, but is instead utilized for DH supply, can perhaps not be considered EH. It could then not be argued that DH supply is an efficient measure to increase the energy efficiency of the industrial plant by heat integration with external utilization areas. Only heat which could not be utilized for CCS, or heat recovered from the CCS plant may in such a case be considered EH suitable for DH supply. Furthermore, in Section 4.1.4 it was concluded that even though a lot of DH was lost in the steel mill case, implementation of CCS resulted in a larger emission reduction than providing DH delivery. Therefore, considering the benefit to the climate, despite the DH loss, prioritizing CCS as in Part 1 is preferred.

When choosing a design and operational mode, it should also be considered how the view on DH supply from industrial plants and CCS may change in the future. In Part 2, two designs and operational modes were considered. In the economic evaluation it was shown that the cost of SV and CL are similar. With the sensitivity analysis taken into account, CL seems to be more economically favorable. However, even though SV results in an oversized plant with unused potential of the plant during most of the year, if the view on the value of CCS were to change in the future, it may be beneficial to invest in an oversized plant. This would provide the opportunity to convert to constant load operation if required by regulations or motivated by a sufficiently high priced cost for emitting $CO_2$. Another factor to consider is how far away from commercial implementation other carbon reducing technologies for a specific industry are. For example, in a situation where the demand on carbon reduction is anticipated to increase gradually, and other carbon reducing technology is expected in a near future, it may be more beneficial to invest in a smaller capture plant.

Another factor which should be considered in relation to Part 2 is the usage of fuel to run the carbon capture plant. In this thesis, natural gas was chosen as fuel as it was deemed likely source of additional heat in the steel mill case. Even though SV and CL have the same $CO_2$ avoidance, the morality of compensating with fossil fuel to prevent $CO_2$ emissions may be questioned. Other fuels, such as biofuels can of course be considered, but the availability may be limited. Additionally, the economic results of Part 2 would in that case change due to different pricing.

To summarize, in the current situation, all options investigated in this thesis in some sense have potential for future implementation. Due to the expense of DH loss, from an economical point of view, the approach with retained DH delivery is the most viable in the current situation. However, from an environmental point of view, comparing the $CO_2$ reduction of CCS and DH, the approach of Part 1 where CCS is prioritized is more favorable, and also the most desirable. Considering the expense of emissions will rise in the future, out of the two operational modes of Part 2, SV is more favorable as it provides more flexibility in terms of future changes in operation. However, ultimately, the most favorable alternative is, now and in the future, dependent on how DH and CCS as carbon emission mitigation strategies and energy efficiency measures will be valued in relation to each other.

# 5
# Conclusion

In this thesis, the heat recovery potential from a solvent-based $CO_2$ separation plant to the district heating network was investigated. A refinery and a steel mill were used as reference cases. It was found that there is potential for heat recovery and that the amount of recoverable heat is dependent on the properties of the flue gas from the specific industry, such as $CO_2$ concentration and temperature. The largest heat recovery potential was found to be that of the stripper top reflux stream. The amount of recoverable heat is however strongly dependent on the stripper reflux temperature, which is affected by the properties of the flue gas. With a minimum temperature difference of 10°C in heat transfer, 9.7% of the heat supplied to the reboiler of the $CO_2$ separation plant could be recovered for district heating for the steel mill case which has a flue gas at low temperature and a high $CO_2$ concentration. For the refinery case, with a flue gas of high temperature and low concentration, 25.5% could be recovered.

Furthermore, two approaches to operating the $CO_2$ separation plant with seasonal variations in excess heat availability were investigated. It was found that the two different approaches, seasonally varying or constant load operation of a $CO_2$ plant operating on excess heat, while still retaining district heating supply, were comparable in costs. Based on the case study of a Swedish steel mill, it was found that the share of $CO_2$ avoided to the total amount of captured $CO_2$ for the seasonally varying operation plant was 99%, while the corresponding share for the constant load operation plant was 93%. From the sensitivity analysis, the constant load operation plant seems to have a lower specific cost in general for the investigated ranges. However, the difference in cost was small, and thus, to invest in an oversized plant, avoiding extensive use of additional fuel as well as allowing for more $CO_2$ capture if required in a future scenario, was concluded the most feasible option from today's point of view.

The distribution of industrial excess heat to CCS and district heating was also evaluated. The option of prioritizing CCS operation over district heating supply was compared to the option of prioritizing a retained district heating supply over capturing as much $CO_2$ as possible. The investigation showed that to size and operate a CCS plant according to the two options results in comparable specific costs. However, mostly due to a large loss in district heating supply, the annualized cost of a plant while prioritizing CCS is significantly higher than if district heating delivery is retained. Economically, operating the CCS plant while retaining the district heat delivery can therefore be considered the most viable option in the current situation. The comparison however depends on the view on CCS and district heating. Today,

district heating is valued highly, however, in the future, CCS and district heating may be valued differently in relation to each other. This is supported by the fact that the emissions reduction in the steel mill case was smaller for district heating than for CCS, and thus, from an emission reduction perspective, to prioritize CCS operation over a retained district heating supply is the preferred choice.

## 5.1 Future work

The future work, taking off where this thesis has ended, could be focused on optimization of the capture plant design, operation and heat integration means with the district heating network. Specifically, possible means to improve heat recovery, such as to more thoroughly evaluate the influence of the process modifications rich-stream split and absorption intercooling, investigate the possibility to use for example heat pumps to raise the temperature of the stripper top reflux stream, and consider other potential heat sources for district heating, such as the reboiler condenser or the hot flue gases, could be investigated. By building a generic case study and performing sensitivity analysis on the effect of different flue gas properties, the study could be generalized.

In the study of seasonal variations in excess heat availability, only two operational modes and designs were evaluated. The complex problem of finding an optimum in terms of size and operation could be another interesting area to investigate further. More sizes should be examined and evaluated. For these sizes, the optimal mode of operation should be investigated and compared. An extended sensitivity analysis treating future energy market scenarios, as well as the shape of the district heating supply curve could provide additional knowledge on the important design factors.

Finally, prioritizing either CCS or district heating completely in a sense describes two extreme approaches to heat integration. Approaches in which for example only part of the excess heat utilized for district heating is re-purposed for utilization in the $CO_2$ separation plant, so that the excess heat is more evenly distributed between the systems may also prove economically feasible, and therefore worth exploring.

# Bibliography


[1] IPCC, *Global Warming of 1.5°C*, 2018. [Online]. Available: https://www.ipcc.ch/sr15/.

[2] IPCC, *Climate Change 2007: The physical science basis, Contribution of Working Group I to the Fourth Assessment Report of the Intergovernmental Panel on Climate Change*, 2007. [Online]. Available: https://www.ipcc.ch/report/ar4/wg1/.

[3] NOAA, *Trends in Atmospheric Carbon Dioxide (2019)*. [Online]. Available: https://www.esrl.noaa.gov/gmd/ccgg/trends/global.html.

[4] "Paris agreement", in *COP21*, United Nations Framework Convention on Climate Change. [Online]. Available: https://unfccc.int/files/essential_background/convention/application/pdf/english_paris_agreement.pdf.

[5] IEA, *Multiple Benefits of Energy Efficiency*, 2019. [Online]. Available: https://www.iea.org/reports/multiple-benefits-of-energy-efficiency.

[6] Energimyndigheten, *District Heating*, 2015. [Online]. Available: http://www.energimyndigheten.se/en/sustainability/households/heating-your-home/district-heating/.

[7] S. Werner, "District heating and cooling in Sweden", *Energy*, vol. 126, pp. 419–429, 2017, ISSN: 0360-5442. DOI: https://doi.org/10.1016/j.energy.2017.03.052. [Online]. Available: http://www.sciencedirect.com/science/article/pii/S0360544217304140.

[8] Naturvårdsverket, *Fördjupad analys av den svenska klimatomställningen 2019: Industrin i fokus*, 2019. [Online]. Available: http://www.naturvardsverket.se/Om-Naturvardsverket/Publikationer/ISBN/6900/978-91-620-6911-7/.

[9] IEA, *The Role of $CO_2$ Storage*, 2019. [Online]. Available: https://www.iea.org/reports/the-role-of-co2-storage.

[10] S. Budinis, S. Krevor, N. M. Dowell, N. Brandon, and A. Hawkes, "An assessment of CCS costs, barriers and potential", *Energy Strategy Reviews*, vol. 22, pp. 61–81, 2018, ISSN: 2211-467X. DOI: https://doi.org/10.1016/j.esr.2018.08.003. [Online]. Available: http://www.sciencedirect.com/science/article/pii/S2211467X18300634.

[11] M. Biermann, F. Normann, F. Johnsson, and R. Skagestad, "Partial Carbon Capture by Absorption Cycle for Reduced Specific Capture Cost", *Industrial & Engineering Chemistry Research*, vol. 57, no. 45, pp. 15 411–15 422, 2018, ISSN: 0888-5885. DOI: 10.1021/acs.iecr.8b02074. [Online]. Available: https://doi.org/10.1021/acs.iecr.8b02074.

[12] F. Normann, R. Skagestad, M. Biermann, J. Wolf, and A. Mathisen, *$CO_2$stCap*, 2019. [Online]. Available: %7Bhttps://www.sintef.no/contentassets/39f1dfcc7a80403580f5f784e16484a2/final-report-co2stcap.pdf%7D.

[13] D. Johansson, J. Sjöblom, and T. Berntsson, "Heat supply alternatives for CO2 capture in the process industry", *International Journal of Greenhouse Gas Control*, vol. 8, pp. 217–232, 2012, ISSN: 1750-5836. DOI: https://doi.org/10.1016/j.ijggc.2012.02.007. [Online]. Available: http://www.sciencedirect.com/science/article/pii/S1750583612000382.

[14] H. Ali, N. H. Eldrup, F. Normann, V. Andersson, R. Skagestad, A. Mathisen, and L. E. Øi, "Cost estimation of heat recovery networks for utilization of industrial excess heat for carbon dioxide absorption", *International Journal of Greenhouse Gas Control*, vol. 74, pp. 219–228, 2018, ISSN: 1750-5836. DOI: https://doi.org/10.1016/j.ijggc.2018.05.003. [Online]. Available: http://www.sciencedirect.com/science/article/pii/S1750583617307545.

[15] V. Andersson, H. Jilvero, P.-Å. Franck, F. Normann, and T. Berntsson, "Efficient Utilization of Industrial Excess Heat for Post-combustion CO2 Capture: An Oil Refinery Sector Case Study", *Energy Procedia*, vol. 63, pp. 6548–6556, 2014, ISSN: 1876-6102. DOI: https://doi.org/10.1016/j.egypro.2014.11.691. [Online]. Available: http://www.sciencedirect.com/science/article/pii/S1876610214025065.

[16] IEA, *Global CO2 emissions by sector, 2017*, 2019. [Online]. Available: https://www.iea.org/data-and-statistics/charts/global-co2-emissions-by-sector-2017.

[17] Ł. Bartela, A. Skorek-Osikowska, and J. Kotowicz, "Economic analysis of a supercritical coal-fired CHP plant integrated with an absorption carbon capture installation", *Energy*, vol. 64, pp. 513–523, 2014, ISSN: 0360-5442. DOI: https://doi.org/10.1016/j.energy.2013.11.048. [Online]. Available: http://www.sciencedirect.com/science/article/pii/S0360544213010189.

[18] S. Broberg Viklund and M. T. Johansson, "Technologies for utilization of industrial excess heat: Potentials for energy recovery and CO2 emission reduction", *Energy Conversion and Management*, vol. 77, pp. 369–379, 2014, ISSN: 0196-8904. DOI: https://doi.org/10.1016/j.enconman.2013.09.052. [Online]. Available: http://www.sciencedirect.com/science/article/pii/S0196890413006134.

[19] L. Olsson, E. Wetterlund, and M. Söderström, "Assessing the climate impact of district heating systems with combined heat and power production and industrial excess heat", *Resources, Conservation and Recycling*, vol. 96, pp. 31–39, 2015, ISSN: 0921-3449. DOI: https://doi.org/10.1016/j.resconrec.2015.01.006. [Online]. Available: http://www.sciencedirect.com/science/article/pii/S0921344915000075.

[20] K. Pettersson, E. Axelsson, L. Eriksson, E. Svensson, T. Berntsson, and S. Harvey, "Holistic methodological framework for assessing the benefits of delivering industrial excess heat to a district heating network", *International Journal of Energy Research*, vol. 44, no. 4, pp. 2634–2651, 2020, ISSN: 0363-907X. DOI: 10.1002/er.5005. [Online]. Available: https://onlinelibrary.wiley.com/doi/abs/10.1002/er.5005.

[21] Statens Offentliga Utredningar, *Vägen till en klimatpositiv framtid*, 2020. [Online]. Available: https://www.regeringen.se/48ec20/contentassets/1c43bca1d0e74d44af84a0e2387bfbcc/vagen-till-en-klimatpositiv-framtid-sou-20204.

[22] D. Bjørnsen, J. Kjærstad, D. Langlet, A. Mathisen, P. Aagaard, and A. Anundskås, *Carbon Capture and Storage in the Skagerrak/Kattegat region*, Report, 2012. [Online]. Available: https://interreg-oks.eu/webdav/files/gamla-projektbanken/se/Material/Files/Kattegat/Skagerrak/Dokumenter+projektbank/CCS%20final%20report.pdf.

[23] B. Metz, O. Davidson, M. de Coninck, and L. Meyer, *Special Report on Carbon Dioxide Capture and Storage Prepared by the Working Group III of the Intergovernmental Panel on Climate Change*, Generic, 2005.

[24] M. Godec, V. Kuuskraa, T. Van Leeuwen, L. Stephen Melzer, and N. Wildgust, "CO2 storage in depleted oil fields: The worldwide potential for carbon dioxide enhanced oil recovery", *Energy Procedia*, vol. 4, pp. 2162–2169, 2011, ISSN: 1876-6102. DOI: https://doi.org/10.1016/j.egypro.2011.02.102. [Online]. Available: http://www.sciencedirect.com/science/article/pii/S1876610211002992.

[25] S. Ó. Garðarsdóttir, F. Normann, R. Skagestad, and F. Johnsson, "Investment costs and CO2 reduction potential of carbon capture from industrial plants – A Swedish case study", *International Journal of Greenhouse Gas Control*, vol. 76, pp. 111–124, 2018, ISSN: 1750-5836. DOI: https://doi.org/10.1016/j.ijggc.2018.06.022. [Online]. Available: http://www.sciencedirect.com/science/article/pii/S1750583617309416.

[26] M. Wang, A. Lawal, P. Stephenson, J. Sidders, and C. Ramshaw, "Post-combustion CO2 capture with chemical absorption: A state-of-the-art review", *Chemical Engineering Research and Design*, vol. 89, no. 9, pp. 1609–1624, 2011, ISSN: 0263-8762. DOI: https://doi.org/10.1016/j.cherd.2010.11.005. [Online]. Available: http://www.sciencedirect.com/science/article/pii/S0263876210003345.

[27] Y. Le Moullec and M. Kanniche, "Screening of flowsheet modifications for an efficient monoethanolamine (MEA) based post-combustion CO2 capture", *International Journal of Greenhouse Gas Control*, vol. 5, no. 4, pp. 727–740, 2011, ISSN: 1750-5836. DOI: https://doi.org/10.1016/j.ijggc.2011.03.004. [Online]. Available: http://www.sciencedirect.com/science/article/pii/S175058361100034X.

[28] K. Stéphenne, "Start-up of World's First Commercial Post-combustion Coal Fired CCS Project: Contribution of Shell Cansolv to SaskPower Boundary Dam ICCS Project", *Energy Procedia*, vol. 63, pp. 6106–6110, 2014, ISSN: 1876-6102. DOI: https://doi.org/10.1016/j.egypro.2014.11.642. [Online]. Available: http://www.sciencedirect.com/science/article/pii/S1876610214024576.

[29] US Energy Information Adminsitration, *Petra Nova is one of two carbon capture and sequestration power plants in the world*, 2017. [Online]. Available: https://www.eia.gov/todayinenergy/detail.php?id=33552#.

[30] S. Ó. Garðarsdóttir, F. Normann, K. Andersson, and F. Johnsson, "Post-combustion CO2 Capture Using Monoethanolamine and Ammonia Solvents: The Influence of CO2 Concentration on Technical Performance", *Industrial & Engineering Chemistry Research*, vol. 54, no. 2, pp. 681–690, 2015, ISSN: 0888-5885. DOI: 10.1021/ie503852m. [Online]. Available: https://doi.org/10.1021/ie503852m.

[31] M. Biermann, H. Ali, M. Sundqvist, M. Larsson, F. Normann, and F. Johnsson, "Excess heat-driven carbon capture at an integrated steel mill – Considerations for capture cost optimization", *International Journal of Greenhouse Gas Control*, vol. 91, p. 102 833, 2019, ISSN: 1750-5836. DOI: https://doi.org/10.1016/j.ijggc.2019.102833. [Online]. Available: http://www.sciencedirect.com/science/article/pii/S1750583619303068.

[32] K. Li, W. Leigh, P. Feron, H. Yu, and M. Tade, "Systematic study of aqueous monoethanolamine (MEA)-based CO2 capture process: Techno-economic assessment of the MEA process and its improvements", *Applied Energy*, vol. 165, pp. 648–659, 2016, ISSN: 0306-2619. DOI: https://doi.org/10.1016/j.apenergy.2015.12.109. [Online]. Available: http://www.sciencedirect.com/science/article/pii/S0306261915016827.

[33] Y. Seo, C. Huh, S. Lee, and D. Chang, "Comparison of CO2 liquefaction pressures for ship-based carbon capture and storage (CCS) chain", *International Journal of Greenhouse Gas Control*, vol. 52, pp. 1–12, 2016, ISSN: 1750-5836. DOI: https://doi.org/10.1016/j.ijggc.2016.06.011. [Online]. Available: http://www.sciencedirect.com/science/article/pii/S1750583616303012.

[34] H. Deng, S. Roussanaly, and G. Skaugen, "Techno-economic analyses of CO2 liquefaction: Impact of product pressure and impurities", *International Journal of Refrigeration*, vol. 103, pp. 301–315, 2019, ISSN: 0140-7007. DOI: https://doi.org/10.1016/j.ijrefrig.2019.04.011. [Online]. Available: http://www.sciencedirect.com/science/article/pii/S0140700719301677.

[35] E. N. Perspective, *Northern Lights show the way to seaborne CCS solutions*, Newspaper Article, 2020. [Online]. Available: https://energynorthern.com/2020/03/20/northern-lights-show-the-way-to-seaborne-ccs-solutions/.

[36] I. GmbH, *Basic steps to compressor unit calculation*, Web Page. [Online]. Available: https://intech-gmbh.com/compr_calculation_and_selection/#compressors_designing.

[37] IEA, *Tracking industry*, Report, 2019. [Online]. Available: https://www.iea.org/reports/tracking-industry.

[38] IEA, *Technology Roadmap - Carbon Capture and Storage in Industrial Applications*, 2011. [Online]. Available: https://www.iea.org/reports/technology-roadmap-carbon-capture-and-storage-in-industrial-applications.

[39] SSAB, *SSAB Luleå Miljörapport*, Report, 2015. [Online]. Available: https://www.ssab.com/download-center?dcFilter=environmentalre&dcSearch=.

[40] *Fjärrvärmen i luleå*, 2020. [Online]. Available: https://www.luleaenergi.se/sv/privatkund/fjarrvarme/fjarrvarme/allmant-om-fjarrvarme/.

[41] *Årets nyckeltal*, 2020. [Online]. Available: https://www.luleaenergi.se/sv/arsredovisning/redovisning2019/granska-oss/arets-nyckeltal/.

[42] *Preemraff Göteborg*. [Online]. Available: https://www.preem.se/om-preem/om-oss/vad-vi-gor/raff/preemraff-goteborg/.

[43] R. Gottfridsson and I. Johansson, "Investigation of the opportunity for heat integration at Preemraff Göteborg", M.Sc, 2011.

[44] Preem AB, *Miljörapport 2018 Preemraff Göteborg*, 2019.

[45] Preem AB, *Preem progress book: sustainability report 2018*, 2019. [Online]. Available: https://www.preem.se/globalassets/om-preem/hallbarhet/hallbarhetsredovisning/preem_progressbook2018_eng.pdf.

[46] D. Johansson, P.-Å. Franck, and T. Berntsson, "CO2 capture in oil refineries: Assessment of the capture avoidance costs associated with different heat supply options in a future energy market", *Energy Conversion and Management*, vol. 66, pp. 127–142, 2013, ISSN: 0196-8904. DOI: https://doi.org/10.1016/j.enconman.2012.09.026. [Online]. Available: http://www.sciencedirect.com/science/article/pii/S0196890412003767.

[47] T. Berntsson, L. Persson Elmeroth, J. Algehed, E. Hektor, P.-Å. Franck, A. Åsblad, F. Johnsson, A. Lyngfelt, B. Gevert, and T. Richards, *Towards Sustainabel Oil Refinery - Pre-study for larger co-operation project*. Chalmers University of Technology, 2008, Accession Number: cpl.69752; Publication Type: Report; Language: English. [Online]. Available: http://search.ebscohost.com/login.aspx?direct=true&AuthType=sso&db=ir01368a&AN=cpl.69752&site=eds-live&scope=site&custid=s3911979&authtype=sso&group=main&profile=eds%20https://research.chalmers.se/publication/69752.

[48] Preem AB, *Miljörapport 2017 Preemraff Göteborg*, 2018.

[49] Göteborg Energi, *Års- och hållbarhetsredovisning 2018*, 2018. [Online]. Available: https://www.goteborgenergi.se/Files/Webb20/BILDER/Bilder%20som%20INTE%20finns%20i%20GE%E2%80%99s%20bildbank/G%C3%B6teborg%20Energi%20%C3%A5rs-%20och%20h%C3%A5llbarhetsredovisning%202018.pdf?TS=636875617561070267.

[50] G. J. Martinez Castilla, "Dynamics of CO2 Capture Integrated in a Steel Mill", M.Sc. 2018. [Online]. Available: https://hdl.handle.net/20.500.12380/255968.

[51] G. Martinez Castilla, M. Biermann, R. M. Montañés, F. Normann, and F. Johnsson, "Integrating carbon capture into an industrial combined-heat-and-power plant: performance with hourly and seasonal load changes", *International Journal of Greenhouse Gas Control*, vol. 82, pp. 192–203, 2019, ISSN: 1750-5836. DOI: https://doi.org/10.1016/j.ijggc.2019.01.015. [Online]. Available: http://www.sciencedirect.com/science/article/pii/S175058361830687X.

[52] Engineering ToolBox, *Combustion of Fuels - Carbon Dioxide Emission*, 2009. [Online]. Available: https://www.engineeringtoolbox.com/co2-emission-fuels-d_1085.html.

[53] M. Mazzoccoli, B. Bosio, and E. Arato, "Analysis and Comparison of Equations-of-State with p--T Experimental Data for CO2 and CO2-Mixture Pipeline

Transport", *Energy Procedia*, vol. 23, pp. 274–283, 2012, ISSN: 1876-6102. DOI: https://doi.org/10.1016/j.egypro.2012.06.052. [Online]. Available: http://www.sciencedirect.com/science/article/pii/S1876610212010922.

[54] G. Towler and R. Sinnott, "Chemical Engineering Design : Principles, Practice and Economics of Plant and Process Design", in. Oxford, UNITED KINGDOM: Elsevier Science & Technology, 2012, ch. 7 Capital Cost Estimating, ISBN: 9780080966601. [Online]. Available: http://ebookcentral.proquest.com/lib/chalmers/detail.action?docID=858659.

[55] M. van der Spek, E. Sanchez Fernandez, N. H. Eldrup, R. Skagestad, A. Ramirez, and A. Faaij, "Unravelling uncertainty and variability in early stage techno-economic assessments of carbon capture technologies", *International Journal of Greenhouse Gas Control*, vol. 56, pp. 221–236, 2017, ISSN: 1750-5836. DOI: https://doi.org/10.1016/j.ijggc.2016.11.021. [Online]. Available: http://www.sciencedirect.com/science/article/pii/S1750583616308404.

[56] S. O. Gardarsdottir, E. De Lena, M. Romano, S. Roussanaly, M. Voldsund, J.-F. Pérez-Calvo, D. Berstad, C. Fu, R. Anantharaman, D. Sutter, M. Gazzani, M. Mazzotti, and G. Cinti, "Comparison of Technologies for CO2 Capture from Cement Production—Part 2: Cost Analysis", *Energies*, vol. 12, no. 3, p. 542, 2019, ISSN: 1996-1073. [Online]. Available: https://www.mdpi.com/1996-1073/12/3/542.

[57] H. Ali, N. H. Eldrup, F. Normann, R. Skagestad, and L. E. Øi, "Cost Estimation of CO2 Absorption Plants for CO2 Mitigation – Method and Assumptions", *International Journal of Greenhouse Gas Control*, vol. 88, pp. 10–23, 2019, ISSN: 1750-5836. DOI: https://doi.org/10.1016/j.ijggc.2019.05.028. [Online]. Available: http://www.sciencedirect.com/science/article/pii/S1750583618309332.

[58] R. M. Montañés, N. E. Flø, and L. O. Nord, "Experimental results of transient testing at the amine plant at Technology Centre Mongstad: Open-loop responses and performance of decentralized control structures for load changes", *International Journal of Greenhouse Gas Control*, vol. 73, pp. 42–59, 2018, ISSN: 1750-5836. DOI: https://doi.org/10.1016/j.ijggc.2018.04.001. [Online]. Available: http://www.sciencedirect.com/science/article/pii/S1750583618300306.

[59] *Nord Pool Historical Market Data: Elspot Prices 2019 Hourly EUR*, 2019. [Online]. Available: https://www.nordpoolgroup.com/historical-market-data/.

[60] D. Romanchenko, E. Nyholm, M. Odenberger, and F. Johnsson, "Balancing investments in building energy conservation measures with investments in district heating – A Swedish case study.", *To be submitted*, 2020.

# A

# Grand composite curves, refinery case

Figure A.1 and A.2 displays the grand composite curves for the Volvo DH network (high temperature network) and the GEAB DH network (low temperature network) respectively, The grand composite curves are based on the data of Berntsson et al., and displays the available heat amount of heat in the network with the DH demand excluded. The amount of heat at sufficient temperature to be utilized for CCS (125°C in shifted temperatures) is marked by the orange line, while the yellow line displays the heat availability above the return temperature of the DH water in each respective network.

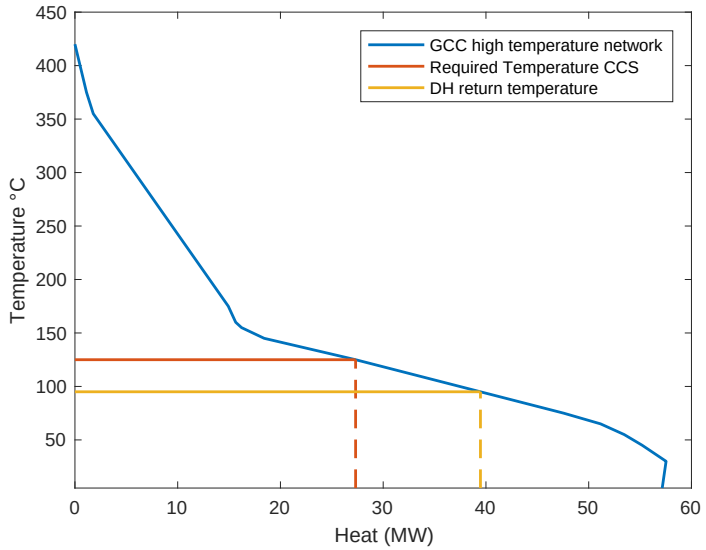


**Figure A.1:** Grand composite curve displaying the heat availability in the high temperature network. The orange line marks the amount of heat at sufficient temperature for CCS (125°C in shifted temperatures), while the yellow line displays the heat availability above the return temperature (95°C in shifted temperatures). Adapted from [47].

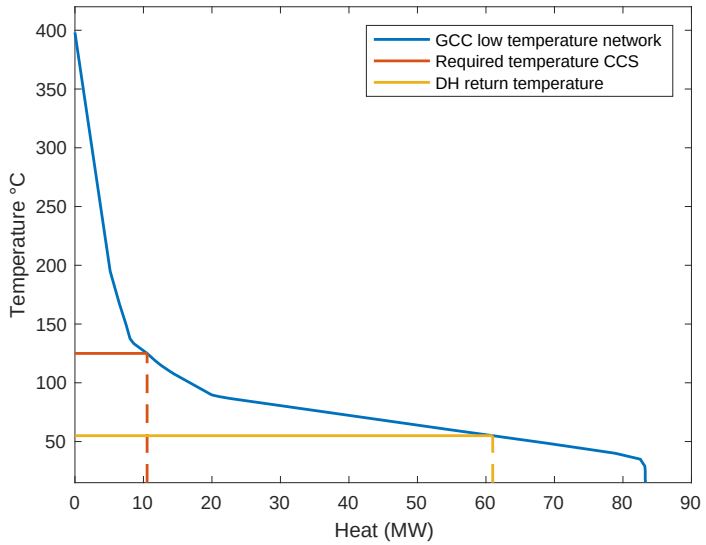


**Figure A.2:** Grand composite curve displaying the heat availability in the low temperature network. The orange line marks the amount of heat at sufficient temperature for CCS (125°C in shifted temperatures), while the yellow line displays the heat availability above the return temperature (55°C in shifted temperatures). Adapted from [47].

# B

# Cost estimation data

Figure B.1 displays the process equipment taken into account in the economic evaluation of the $CO_2$ separation plant, including 3 tanks 8 pumps and 6 heat exchangers. Other process equipment which was also included in the economic evaluation, but not displayed in the scheme, are a cooling water pump and filters.

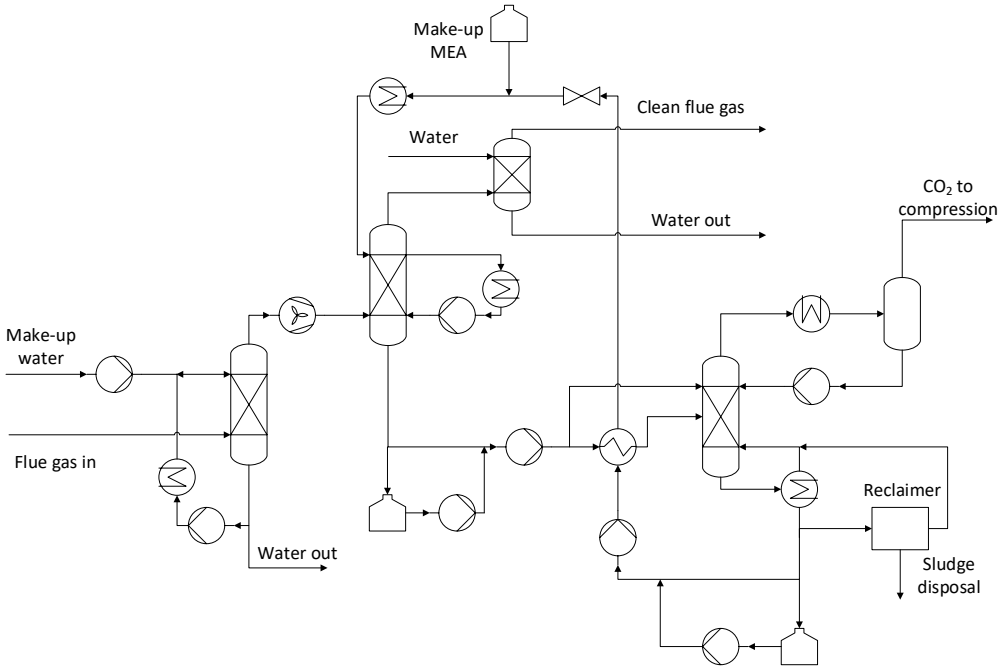


**Figure B.1:** A process scheme displaying all equipment in the separation plant taken into account in the economic evaluation [31].

## B.1 Power-law cost functions

The cost data used to evaluate the equipment cost was collected from several sources treating similar plants [31], [55], [56]. The cost of each piece of equipment collected from literature was corrected to a common costing year (2015) by using the Chemical Engineering Plant Cost Index (CEPCI). The costs were then plotted against the correct sizing parameter (Table 3.5) for each piece of equipment, and an equipment type specific power-law cost function was obtained. The data points collected from literature along with the fitted power-law cost functions are shown in Figure B.2 to

B.7. The cost functions display costs in 2015 prices, and have to be converted to the desired costing year, by using a suitable index.

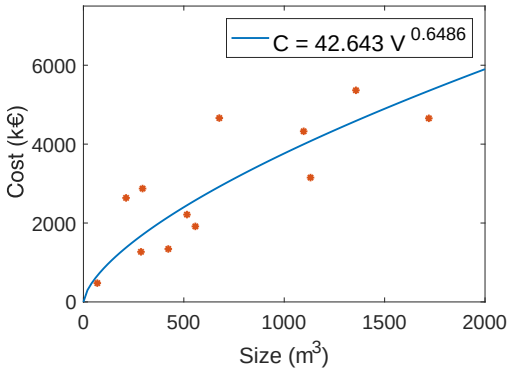


**Figure B.2:** Cost function, columns with internals, welded stainless steel (SS316).

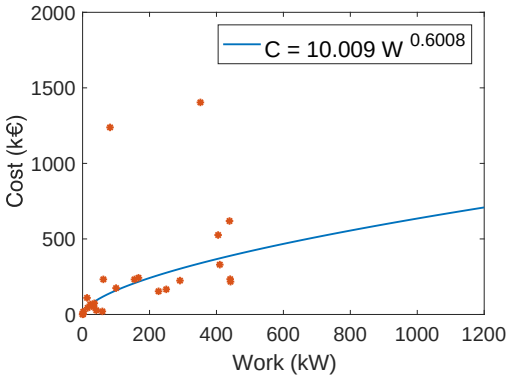


**Figure B.3:** Cost function, pumps, machined stainless steel (SS316).

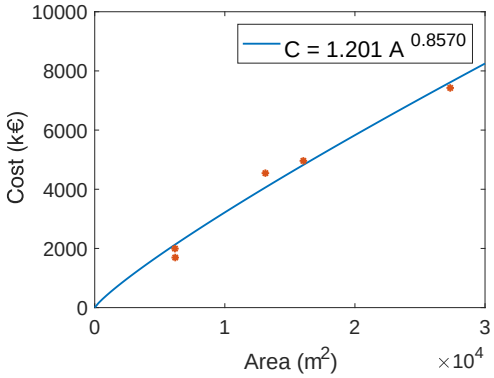


**Figure B.4:** Cost function, reboiler, welded stainless steel (SS316).

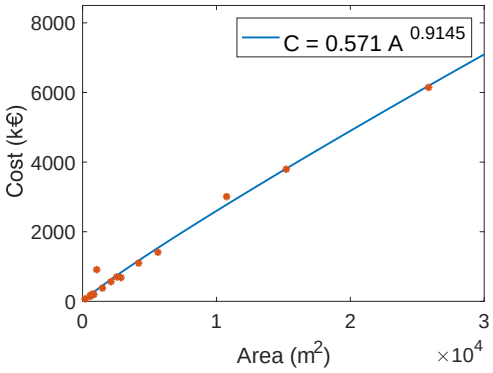


**Figure B.5:** Cost function, other heat exchangers, welded stainless steel (SS316).

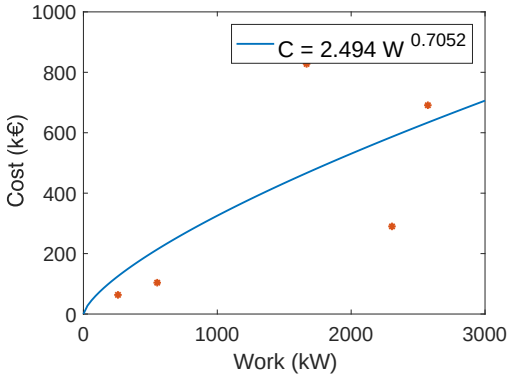


**Figure B.6:** Cost function, flue gas fan, carbon steel (CS).

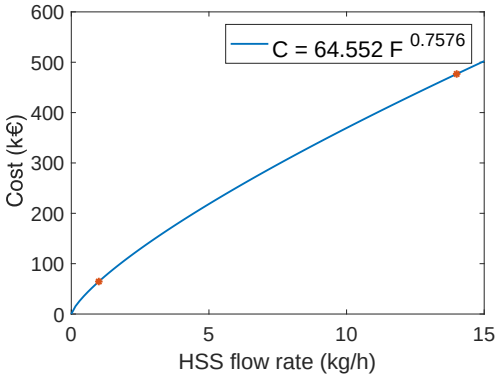


**Figure B.7:** Cost function, reclaimer, welded stainless steel (SS316).

## B.2 EDF factors equipment cost

In table 9, the cost factors of the EDF method are shown. The cost factors are obtained from the paper by Ali et al. [57].

,

**Table B.1:** EDF cost factors by equipment cost, adapted from [57].

| Cost of equipment (kNOK,CS) | 0–20 | 20–100 | 100–500 | 500–1000 | 1000–2000 | 2000–5000 | 5000–15000 | >15000 |
|---|---|---|---|---|---|---|---|---|
| **Direct cost components** | | | | | | | | |
| Equipment | 1 | 1 | 1 | 1 | 1 | 1 | 1 | 1 |
| Erection/Installation | 0.89 | 0.47 | 0.25 | 0.18 | 0.14 | 0.11 | 0.1 | 0.08 |
| Piping ($f_{piping}$ | 3.56 | 1.92 | 1.12 | 0.83 | 0.65 | 0.48 | 0.41 | 0.29 |
| Electric | 1.03 | 0.71 | 0.48 | 0.41 | 0.34 | 0.28 | 0.25 | 0.18 |
| Instrument | 3.56 | 1.92 | 1.12 | 0.83 | 0.65 | 0.48 | 0.41 | 0.29 |
| Civil | 0.55 | 0.36 | 0.25 | 0.2 | 0.17 | 0.14 | 0.13 | 0.09 |
| Steel & Concrete | 1.79 | 1.17 | 0.79 | 0.64 | 0.55 | 0.43 | 0.39 | 0.28 |
| Insulation, | 0.67 | 0.34 | 0.18 | 0.14 | 0.11 | 0.09 | 0.05 | 0.04 |
| **Total ($f_{direct}$)** | 13.04 | 7.88 | 5.19 | 4.21 | 3.6 | 3.02 | 2.74 | 2.24 |
| **Engineering cost components** | | | | | | | | |
| Engineering Process | 1.23 | 0.43 | 0.24 | 0.18 | 0.15 | 0.13 | 0.11 | 0.09 |
| Engineering Mechanical | 0.98 | 0.24 | 0.1 | 0.05 | 0.04 | 0.03 | 0.01 | 0.01 |
| Engineering Piping | 1.08 | 0.58 | 0.34 | 0.25 | 0.18 | 0.14 | 0.13 | 0.09 |
| Engineering Electric | 1.04 | 0.3 | 0.15 | 0.11 | 0.1 | 0.09 | 0.05 | 0.04 |
| Engineering Instrument | 1.85 | 0.72 | 0.36 | 0.25 | 0.2 | 0.14 | 0.13 | 0.09 |
| Engineering Civil | 0.39 | 0.11 | 0.04 | 0.03 | 0.03 | 0.01 | 0.01 | 0.01 |
| Engineering Steel & Concrete | 0.58 | 0.24 | 0.13 | 0.1 | 0.09 | 0.05 | 0.05 | 0.04 |
| Engineering Insulation | 0.27 | 0.09 | 0.03 | 0.01 | 0.01 | 0.01 | 0.01 | 0.01 |
| **Total ($f_{eng}$)** | 7.43 | 2.73 | 1.38 | 0.99 | 0.8 | 0.6 | 0.51 | 0.38 |
| **Administration cost components** | | | | | | | | |
| Procurement | 1.55 | 0.52 | 0.2 | 0.13 | 0.09 | 0.04 | 0.03 | 0.03 |
| Project Control | 0.37 | 0.14 | 0.05 | 0.04 | 0.04 | 0.03 | 0.03 | 0.03 |
| Site Management | 0.66 | 0.42 | 0.28 | 0.24 | 0.2 | 0.17 | 0.15 | 0.11 |
| Project Management | 0.89 | 0.46 | 0.29 | 0.24 | 0.2 | 0.17 | 0.15 | 0.11 |
| **Total ($f_{adm}$)** | 3.47 | 1.54 | 0.83 | 0.65 | 0.53 | 0.39 | 0.36 | 0.28 |
| **Commissioning ($f_{com}$)** | 0.72 | 0.33 | 0.17 | 0.1 | 0.1 | 0.05 | 0.05 | 0.04 |
| **Total Known Cost** | 24.66 | 12.48 | 7.57 | 5.95 | 5.03 | 4.06 | 3.66 | 2.94 |
| **Contingency ($f_{cont}$)** | 4.99 | 2.55 | 1.57 | 1.24 | 1.06 | 0.87 | 0.78 | 0.64 |
| **Total Plant Cost ($f_{total}$)** | 29.65 | 15.03 | 9.13 | 7.2 | 6.1 | 4.93 | 4.44 | 3.59 |

# C

# CAPEX estimation Part 2

In Figure C.1 the fitted cost curve obtained from the CAPEX evaluation of the three sizes of the steel mill case are shown. The curve was used to evaluate the CAPEX of the two designs in Part 2. The flue gas flow and calculated CAPEX of the plants of Part 2 are presented in Table C.1.

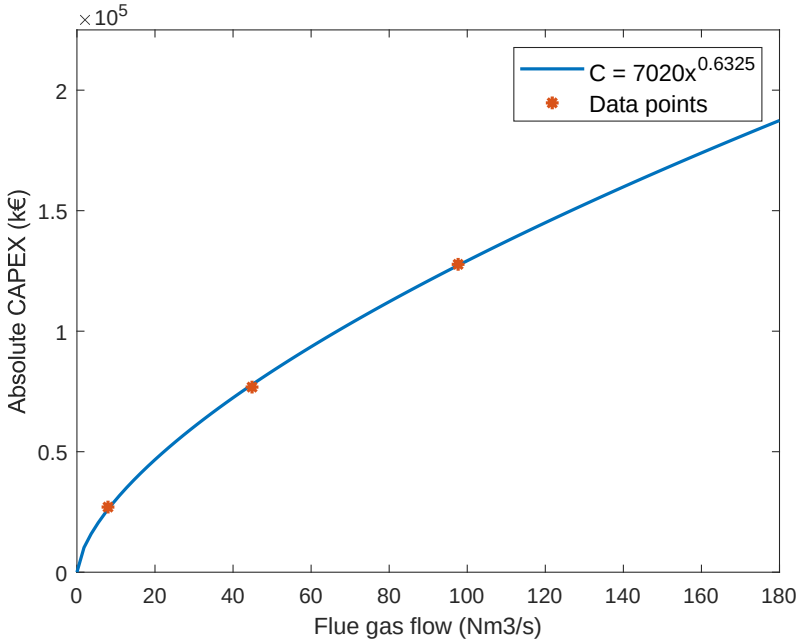


**Figure C.1:** Absolute CAPEX as a function of flue gas flow for the three sizes evaluated for the steel mill case, cost year 2016.

**Table C.1:** Flue gas flow and calculated absolute CAPEX of SV plant and CL plant.

| | **SV** | **CL** |
|---|---|---|
| Flue gas flow ($Nm^3/s$) | 91.6 | 47.9 |
| Absolute CAPEX (k€) | 122,239 | 81,153 |